



Defence Research and
Development Canada

Recherche et développement
pour la défense Canada



Design of a Microstrip Fed Circularly Polarised Printed Antenna for an AEHF Phased Array

*Improving impedance bandwidth of printed radiating
antennas using the proximity coupling technique*

Michel Clénet

Defence R&D Canada – Ottawa

TECHNICAL MEMORANDUM

DRDC Ottawa TM 2004-138

June 2004

Canada

Design of a Microstrip Fed Circularly Polarised Printed Antenna for an AEHF Phased Array

Improving impedance bandwidth of printed radiating antennas using the proximity coupling technique

Michel Clénet

Defence R&D Canada – Ottawa

TECHNICAL MEMORANDUM

DRDC Ottawa TM 2004-138

June 2004

© Her Majesty the Queen as represented by the Minister of National Defence, 2004

© Sa majesté la reine, représentée par le ministre de la Défense nationale, 2004

Abstract

This document reports the study of a circularly polarized printed antenna realised with low temperature co-fired ceramic (LTCC) material. This antenna is developed as a radiating element for a phased array with tile architecture for advanced EHF communication systems. Due to constraints imposed by the LTCC fabrication process and the application, techniques to improve the impedance bandwidth have been applied. These techniques are based on the proximity coupling of resonant structures to the driven antenna. The impedance bandwidth has been improved by a factor 5, and the required bandwidth for advanced extremely high frequency (AEHF) communications has been obtained. Arrays of four optimized radiating elements have been studied. The results are not satisfactory throughout the bandwidth, mainly due to the radiation of the microstrip feeding system required to generate the circular polarization. Another radiating element should be developed with a design suitable for an array for AEHF communications. A solution using the aperture-coupled technique to feed the radiating element can be applied to achieve this goal.

Résumé

Ce document décrit l'étude d'une antenne imprimée à polarisation circulaire réalisée sur un matériau LTCC (low temperature co-fired ceramic). Cette antenne est utilisée comme élément rayonnant d'un réseau à déphasage ayant une architecture de type "tuile", pour des systèmes de communication en bande AEHF (advanced extremely high frequency). A cause de contraintes imposées par le procédé de fabrication LTCC, plusieurs techniques d'élargissement de la bande passante sont utilisées. Ces techniques sont basées sur le couplage de proximité de structures résonnantes. La bande passante a ainsi été améliorée par un facteur 5, et la bande passante requise pour les communications en bande AEHF a été obtenue. Des réseaux de quatre éléments ont été étudiés. Les résultats obtenus ne sont pas satisfaisants sur toute la bande de fréquence, principalement à cause du rayonnement du système d'alimentation en lignes microruban nécessaire à l'obtention de la polarisation circulaire. Un nouvel élément rayonnant pouvant être utilisé en réseau pour des communications en bande AEHF devra être développé. Une solution consisterait à utiliser la technique de couplage par ouverture pour alimenter l'antenne.

This page intentionally left blank.

Executive summary

The requirement for greater bandwidth in military satellite communication systems has resulted in research for systems that can be used in the Extremely High Frequency (EHF) band. To support this requirement, the Department of National Defence has sponsored the development of a unique Canadian technology under the Canadian Military Satellite Communications (CMSC) Project. This is part of the Canadian commitment to the United States Advanced Extremely High Frequency (AEHF) Military Satellite Communications project. The end goal is to provide the Canadian Military with worldwide military satellite communications to support Canadian Forces operations.

The study reported in this document concerns the analysis of an antenna element suitable for an array with tile architecture operating in the AEHF band. LTCC, low temperature co-fired ceramic, has been selected as the system packaging technology. This technology used extensively in industry, enables the packaging of the different components of a phased array on a same board. A circularly polarized antenna realised in printed technology has been designed considering constraints imposed by the packaging technology (LTCC), and by the application (an array at 20.7 GHz for Advanced EHF communications). The impedance bandwidth of a conventional square patch antenna has been improved from 1% to 3.5% when a 0.214 mm thick substrate is considered, and to 5.1% when a 0.321 mm thick substrate is used. The bandwidth enhancement technique used is based on the addition of resonators on different layers coupled to the driven patch. The radiation characteristics of the radiating element are relatively good in the lower and centre parts of the bandwidth in terms of half-power beamwidth, and axial ratio as well, but they are significantly below the requirements in the upper part of the frequency band. Two arrays of four elements have also been investigated. The results in terms of radiation characteristics of an array of four circularly polarized (CP) elements are compared to the results of an array of four linearly polarized elements arranged in a sequential rotation to obtain the circular polarization. The array with CP elements exhibits better performance, especially in terms of axial ratio.

As the results in terms of radiation characteristics are not constant throughout the bandwidth, another radiating element should be developed with a design suitable for an array for AEHF communications. In particular, the radiation from the feeding system, required to generate the circular polarization, must be minimized to avoid interference with the antenna radiation. A solution using the aperture-coupled technique can be applied to achieve this goal.

Michel Clénet. 2004. Design of a microstrip fed circularly polarized printed antenna for an AEHF phased array. DRDC Ottawa TM 2004-138. Defence R&D Canada - Ottawa.

Sommaire

La demande d'élargissement de la bande passante pour les communications militaires par satellite a engendré l'étude de systèmes de communications opérant en bande EHF. Le Département de la Défense Nationale a donc initié le développement d'une technologie canadienne unique dans le cadre d'un projet de réalisation de systèmes de communications militaires canadiennes par satellite. Ce projet canadien est une partie intégrante du projet américain de communications militaires par satellite en bande EHF, appelé AEHF SatCom.

L'étude reportée dans ce document décrit l'analyse d'une antenne élémentaire pouvant être utilisée dans réseau à déphasage ayant une architecture de type "tuile" fonctionnant en bande EHF. La technologie LTCC, « low temperature co-fired ceramic », a été choisie comme technologie d'intégration. Cette technologie est beaucoup utilisée dans le secteur de l'industrie, et elle permet notamment d'intégrer les différents composants d'un réseau à déphasage. Une antenne élémentaire à polarisation circulaire réalisée en technologie imprimée a été développée en tenant compte des contraintes imposées par la technologie LTCC et par l'application visée (système de communications à 20.7 GHz). La bande passante en terme d'impédance d'une antenne imprimée conventionnelle a été augmentée de 1% à 3.5% en utilisant un substrat de 0.214mm d'épaisseur et à 5.1% en utilisant un substrat de 321 mm d'épaisseur. La technique utilisée pour augmenter la bande passante est basée sur l'addition de résonateurs sur des couches différentes du résonateur alimente. Les caractéristiques de rayonnement de l'antenne élémentaire sont relativement bonnes dans les parties basse et centrale de la bande de fréquences, mais ne rencontrent pas les spécifications dans la partie haute. Deux réseaux de quatre éléments ont également été étudiés. Le premier est composé d'élément à polarisation circulaire et le deuxième d'éléments à polarisation linéaire orientés selon une rotation séquentielle pour obtenir la polarisation circulaire. La comparaison de ces deux réseaux en terme de caractéristiques de rayonnement montre que le réseau premièrement cité possède de meilleures performances.

Néanmoins, comme les caractéristiques désirées n'ont pas été obtenues sur toute la bande de fréquences, un autre élément rayonnant devra être développé. Le rayonnement du système d'alimentation nécessaire à l'obtention de la polarisation circulaire devra être minimisé afin d'éviter toute interférence avec le rayonnement propre de l'antenne. Une solution consiste en l'utilisation de la technique de couplage par une ouverture dans le plan de masse pour alimenter l'antenne élémentaire.

Michel Clénet. 2004. Design of a microstrip fed circularly polarized printed antenna for an AEHF phased array. DRDC Ottawa TM 2004-138. R & D pour la défense Canada - Ottawa

Table of contents

Abstract	i
Résumé	i
Executive summary.....	iii
Sommaire	iv
Table of contents.....	v
List of figures.....	vii
List of tables.....	ix
1. Introduction.....	1
1.1. Goal.....	1
1.2. LTCC Technology	1
1.3. Antenna considerations.....	3
2. Constraints due to the LTCC process	6
3. Design of the antenna on a two-layer substrate	8
3.1. Characteristics of a single square patch	8
3.2. Square patch stacked with a printed ring resonator	10
3.3. Patch radiator stacked with a printed ring resonator and parasitic elements	12
4. Design of the antenna on a three-layer substrate	15
4.1. Preliminary investigations	15
4.2. The final radiating element	17
4.3. The feeding system	20
5. Arrays of four radiating elements	23
6. Concluding remarks	28
7. References.....	29
8. Annexes	30
8.1. Annex 1: LTCC technology.....	30

8.2.	Annex 2: Microstrip line impedance versus substrate thickness and line width.....	32
8.3.	Annex 3: impedance bandwidth enhancement of a patch with an inset feed.....	33
8.4.	Annex 4: Summary of the element dimensions for radiating elements on three-layer LTCC substrate	38

List of figures

Figure 1. Examples of LTCC realisations.....	1
Figure 2. LTCC fabrication process.....	2
Figure 3. LTCC design capabilities	3
Figure 4. Array architectures	4
Figure 5. Schematic of a microstrip patch antenna.....	5
Figure 6. Parameters affected by the LTCC process.....	6
Figure 7. Square patch antenna a) edge fed, b) with inset feed c) edge fed with two quarter-wavelength transformers	8
Figure 8. Input impedance of the patch antenna with inset feed.....	9
Figure 9. CP configuration of the square patch antenna a) with inset feeds and b) edge fed with two quarter-wavelength transformers.....	9
Figure 10. Input impedance of the patch antenna with two quarter-wavelength transformers with one and two ports	10
Figure 11. Patch antenna stacked with a square ring resonator	11
Figure 12. Input impedance of the patch antenna stacked with a square ring resonator.....	11
Figure 13. Patch antenna stacked with a ring resonator and coupled to parasitic elements.....	13
Figure 14. Input impedance of the patch antenna stacked with a ring resonator and coupled to parasitic elements	14
Figure 15. Input impedance of the single patch, the patch stacked with a ring, and a patch stacked with a ring coupled to parasitic elements, fed by a single port	15
Figure 16. Two-port patch antenna stacked with a ring resonator and coupled to parasitic elements on a three-layer substrate.....	16
Figure 17. Input impedance of the patch stacked with a ring, and a patch stacked with a ring coupled to parasitic elements, fed by two ports	17
Figure 18. Two-port patch antenna stacked with two ring resonators and coupled to parasitic elements ..	18
Figure 19. Input impedance of the two-port patch antenna stacked with two ring resonators and coupled to parasitic elements	18
Figure 20. Radiation patterns in circular polarisation and axial ratio of the two-port patch antenna stacked with two ring resonators and coupled to parasitic elements.....	19

Figure 21. Circularly polarized multi-resonators antenna.....	20
Figure 22. Input impedance of the final antenna with and without its feeding circuit.....	20
Figure 23. Radiation patterns and axial ratios of the antenna with its feeding circuit.....	21
Figure 24. Array with a) four circularly polarized antennas and b) four linearly polarized antennas	23
Figure 25. Radiation patterns of the arrays with a) CP radiating elements and b) LP radiating elements..	25
Figure 26. Axial Ratios of the arrays with a) CP radiating elements and b) LP radiating elements.....	26
Figure 27. Patch antenna stacked with a square ring resonator	33
Figure 28. Input impedance of the inset fed patch antenna stacked with a square ring resonator	33
Figure 29. Geometry of the driven patch and the stacked square ring.....	34
Figure 30. Patch antenna stacked with a ring resonator and coupled to parasitic elements.....	36
Figure 31. Input impedance of the patch antenna stacked with a ring resonator and coupled to parasitic elements	37
Figure 32. Radiating element with the transformer (a) and with the complete feeding circuit (b).....	40

List of tables

Table 1	: Summary of the radiation characteristics of the two-port patch antenna stacked with two ring resonators and coupled to parasitic elements	19
Table 2	: Summary of the radiation characteristics of the antenna with its feeding system at 20.7 GHz	22
Table 3	: Summary of the radiation characteristics of the array of four circularly polarized radiating elements at 20.2 GHz	27
Table 4	: Summary of the radiation characteristics of the array of four circularly polarized radiating elements at 20.7 GHz	27
Table 5	: Summary of the radiation characteristics of the array of four linearly polarized radiating elements at 20.7 GHz	27
Table 6	: LTCC Manufacturers and Process Characteristics	30
Table 7	: Process Characteristics	31
Table 8	: Characteristics impedance versus line width for a two-layer LTCC substrate	32
Table 9	: Characteristics impedance versus line width for a three-layer LTCC substrate	32
Table 10	: Dimensions of the resonating elements, and impedance bandwidth of antennas with a single feed	38
Table 11	: Dimensions of the resonating elements, and impedance bandwidth of antennas with two feeds	39
Table 12	: Dimensions of the resonating elements, and impedance bandwidth of the antennas with the feeding system	40

This page intentionally left blank.

1. Introduction

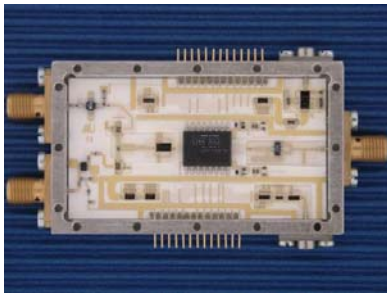
1.1. Goal

The goal of this project is to realize an antenna element suitable for an array with tile architecture. The application of the array is AEHF satellite communications. The antenna must therefore operate with circular polarisation at 20.7 GHz or 44.5 GHz, with a 5% bandwidth.

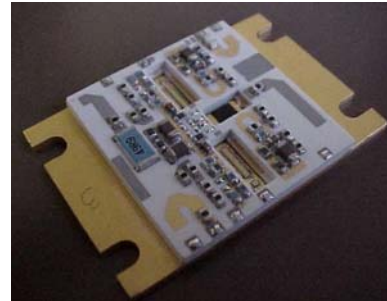
LTCC, low temperature co-fired ceramic, has been selected as the system packaging technology. This technology used extensively in industry, enables the packaging of the different components of a phased array on a same board. It is also still under development for high frequency applications. This technology is briefly summarised in the next section.

1.2. LTCC Technology

LTCC is a multi-layer material used for system packaging. It offers many advantages in high-density integration for RF to millimetre-wave integrated circuits [1]. It is therefore an attractive technology for packaging phased array modules, when the size is an important issue, especially at millimetre-wave frequencies [2]. Circuits realised with other processes, such as GaAs MMICs (monolithic microwave integrated circuits), are assembled in a multi-layer configuration using printed lines, vias and even ball grid arrays (BGA). Figure 1 shows some examples of devices realised in LTCC technology.



Point-to-multipoint transceiver for 24.5 to 26.5 GHz (Source: IMST, Germany)



LTCC RF power amplifier module for base station applications

Source: "RF and Microwave Components in LTCC",
L. Devlin, G. Pearson, J. Pittock - Plextek Ltd.
B. Hunt - CMAC Micro Technology, April, 2001



Source:
<http://www.dilabs.com/Dipak/benefits/1dipak.htm>

Figure 1. Examples of LTCC realisations

This process is called low temperature because the firing temperature is below 1000° Celcius (850° Celcius precisely). This is a great advantage compared to other processes because low loss conductors, such as silver and gold, can be used as their melting temperatures are above the LTCC firing

temperature. Some LTCC materials are also low loss, even at high frequency. DuPont for instance, offers a LTCC tape with 0.002 loss tangent at 40 GHz.

The LTCC fabrication process is described in Figure 2. From a rolled dielectric tape, the layers are first cut and dried. The layers are then perforated where connections between transmission lines on different layers are needed. The cylindrical holes are filled with metal to ensure reliable contacts. The next step is the conductor printing on each separated layer. Then comes the collating step, followed by lamination that is realised with controlled pressure. Finally, the single piece of material is fired at a peak temperature of 850° Celcius. The post-processing operation involves the insertion of the different components by direct soldering, using wire bonding or ball grid array (BGA), as shown in Figure 3.

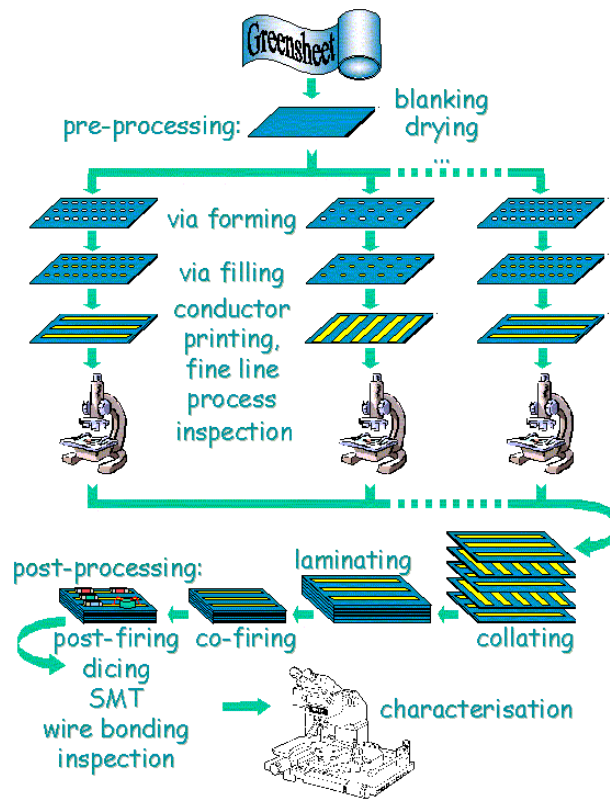


Figure 2. LTCC fabrication process

This brief description summarises a process that must be precise to realize a circuit with characteristics close to those expected. For instance, the lamination is performed with a specific pressure for a precise duration. The firing step is also controlled in temperature and time. Detailed information can be obtained from the material providers [3]-[7].

The LTCC material we are considering is provided by DuPont [3]. DuPont offers several LTCC green tapes. The Dupont 943 tape is the most suitable to RF applications. This tape has a 107 µm fired thickness. Its dielectric permittivity is 7.05 and its loss tangent is 0.002.

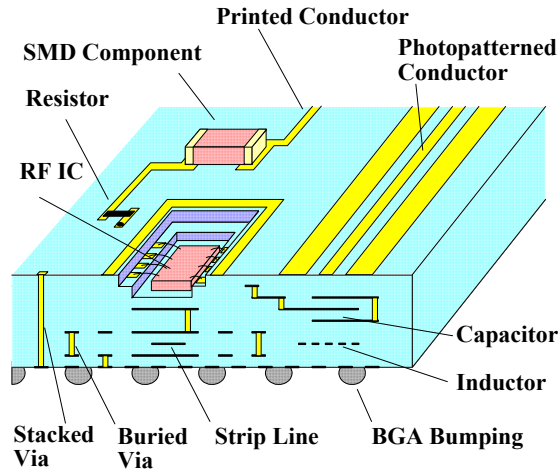


Figure 3. LTCC design capabilities

1.3. Antenna considerations

There are basically two kinds of array architectures, brick architecture and tile architecture. As described in [8], the tile architecture is a multi-layer assembly of the different components of the phased array. The radiating elements, usually printed antennas, are on the top layer. The amplifiers are on a layer below, and then come the phase shifters on a lower layer. With the brick architecture, the array is divided into modules realised on separated boards. Each module contains the radiating element (end-fire type), the amplifier, the phase shifter, filter, and other components. All modules are juxtaposed to form the complete phased array.

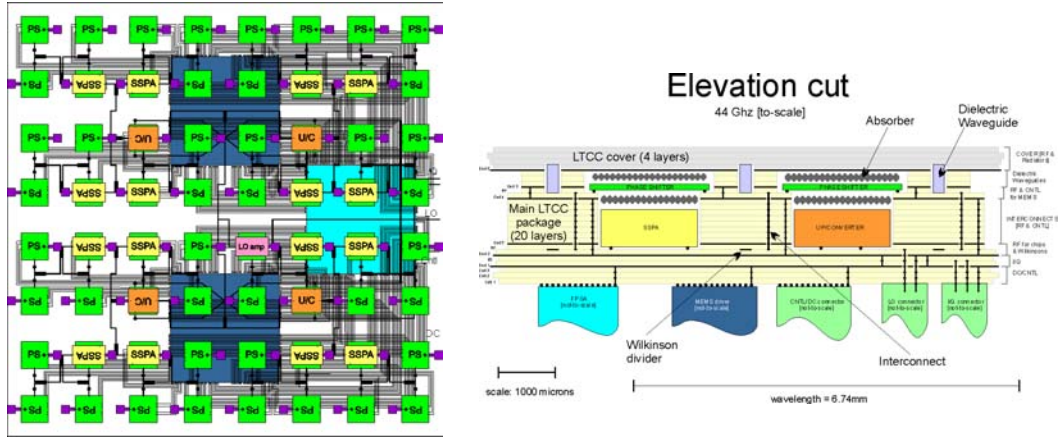
With different kinds of array architectures come different kinds of radiating elements. The printed antennas, like the patch antenna shown in Figure 4 (a patch antenna has a direction of radiation normal to their geometry) are suitable for arrays with a tile architecture whereas the end-fire antennas, whose radiation direction is the prolongation of the antenna structure, are preferred for arrays with a brick architecture.

Circularly polarized antennas are required for AEHF communications. This can be easily obtained with a patch antenna by using two feeds exciting two orthogonal modes with a 90° phase shift. However, as a single access is required, a feeding circuit, integrated into the structure, needs to be designed.

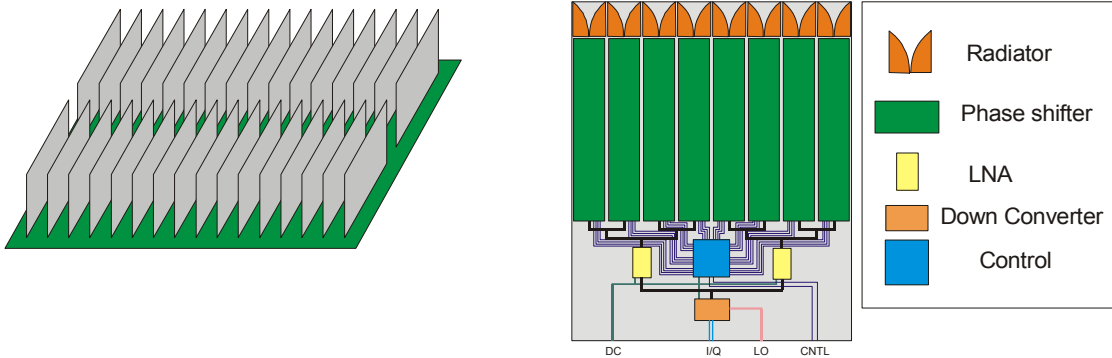
As the patch will be fabricated on a dielectric substrate, surface waves can be significantly excited if the antenna is not designed properly. This will result in a gain loss, and also in an increase in the unwanted mutual coupling when this element is implemented in array configuration. Page 46 of Reference [9] gives a boundary for the height h of the substrate to avoid too much loss due to the excitation of the surface waves:

$$(1) \quad \frac{h}{\lambda_o} \leq \frac{0.3}{2\pi\sqrt{\epsilon_r}}$$

where h is the substrate thickness, λ_o is the wavelength in the free-space, and ϵ_r is the relative permittivity of the material.



a) Array with tile architecture



b) Array with brick architecture

Figure 4. Array architectures

The antenna is designed considering the DuPont 943 LTCC material [3], whose dielectric permittivity is 7.05. Using Equation (1), the maximum substrate thickness must be smaller than $0.018\lambda_0$. This corresponds to a thickness of 0.261 mm at 20.7 GHz, and 0.121 mm at 44.5 GHz. On the other hand, a 5% bandwidth is required for AEHF communications. The impedance bandwidth of a conventional patch, as well as the excitation of the surface waves, depends on the thickness of the dielectric substrate [9], amongst other parameters. For the thickness mentioned above, a bandwidth of about 1% is expected. This result is too far from the AEHF communication requirements. Some solutions to improve the bandwidth without increasing the substrate thickness have to be considered, keeping also in mind that the radiating element area should be no more than $0.5\lambda_0 \times 0.5\lambda_0$ for its use in array configuration. These constraints have to be considered for designing the radiating element, along with the constraints imposed by the LTCC process.

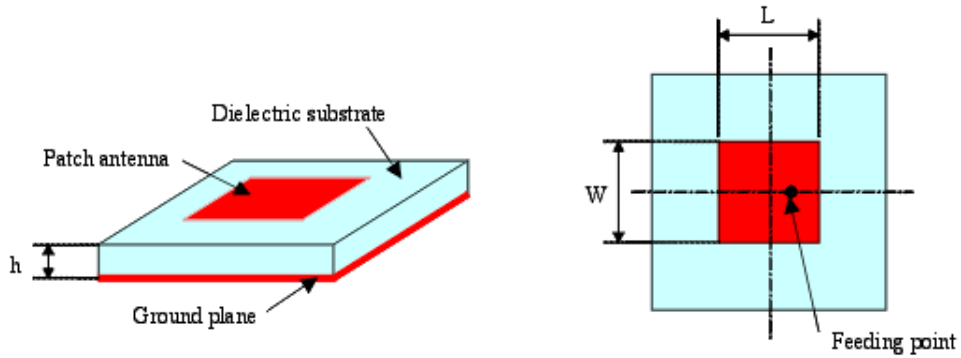


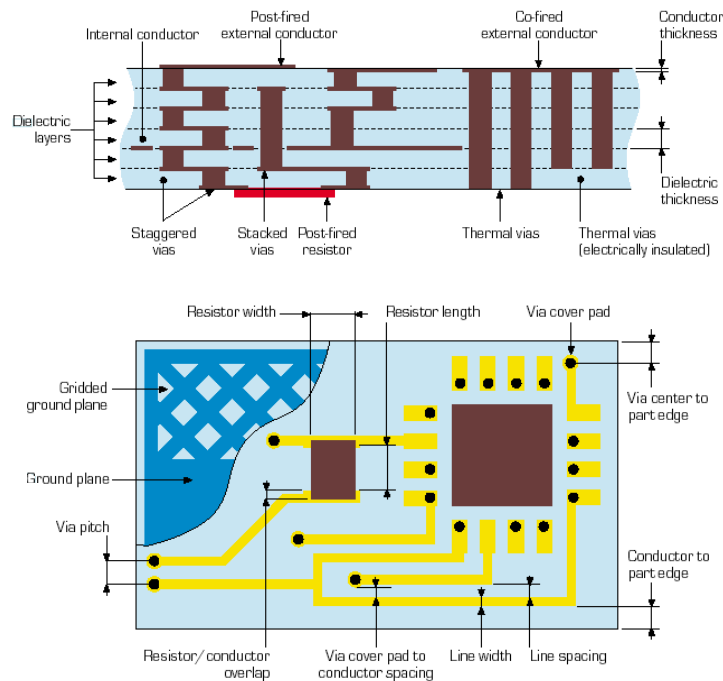
Figure 5. Schematic of a microstrip patch antenna

Printed antennas can have different shapes. The common shapes are square (Figure 5), rectangular, circular, triangular and ellipsoid shapes (see [9], page 9). For this study, a printed antenna with symmetric geometry along the X and Y-axis is considered, as symmetrical radiation patterns in both E- and H-planes are required for circular polarisation. The square patch is preferred to the circular patch for several reasons ([9], pages 354-365). In its fundamental mode, the half-power beamwidth in the E- and H-planes are very close, therefore better axial ratio can be achieved. Also, the square patch antenna has a larger impedance bandwidth than the circular patch. The square patch is therefore the radiating element adopted for this project.

2. Constraints due to the LTCC process

As mentioned previously in the introduction, the LTCC process must follow a number of fabrication steps with a lot of care to achieve the desired design. Only several companies in the world have the tools and the knowledge to fabricate circuits using this technology. The most important ones are listed in Annex 8.1. page 30. Also, LTCC fabrication imposes constraints on the design. The constraints depend on the LTCC material itself, and also on the tools used for fabrication. The main constraints for different LTCC materials and manufacturers are listed in Annex 8.1. page 30. In this section, we will focus on the constraints imposed by our LTCC process manufacturer, VTT, which will affect our design. Their complete design guideline is available online [10]. Figure 6 summarizes the main parameters affected by those constraints.

First, the thickness of the LTCC sheet is fixed and equals $107\ \mu\text{m}$ after co-firing. A minimum of five layers is required to have a rigid substrate, and the LTCC material size can be up to $114 \times 114\ \text{mm}^2$ ($4.5'' \times 4.5''$). The minimum line width is $100\ \mu\text{m}$, as is the minimum line spacing. The maximum line width is $1.5\ \text{mm}$ with unlimited length. The use of 90° -bend lines is recommended for optimum line width control, but 45° -bend lines are allowed. The printed lines must be at least $380\ \mu\text{m}$ from the substrate edge.



Source (drawings): Thales Microsonics

Figure 6. Parameters affected by the LTCC process

Buried large metallic planes, such as ground plane, can not be realised. With large metallic planes, the dielectric sheets on both side are not in contact, and therefore there is a risk of de-lamination of the substrate. Therefore, gridded metallic planes replace filled ones. The grid pattern must cover less than 50% of the area with metallisation. As mentioned in the guideline, the preferred plane uses $250\ \mu\text{m}$ lines

and 550 μm spaces. Note that solid conductor areas in the gridded plane can be used locally to improve RF performance.

Cavities in the substrate can be realised, but their geometrical characteristics must also follow some guidelines. First, the cavity floor must have a minimum fired thickness of 380 μm . This corresponds to a minimum of four layers. The cavity walls must be at least 3.0 mm apart. Any printed line in the cavity must be at least at 200 μm from the cavity walls. The printed lines outside must be at least 250 μm from the cavity walls. Also, any vias must be at a distance of 2.5 times their diameter from the cavity wall.

A guideline for vias (metallised holes) also exists. Vias can go through one layer at a time. Stacking of vias can be done, but this results in a bump on the surface. To avoid this, staggering of vias is recommended. Vias should then be staggered for connection between layers far apart. The minimum via diameter is 150 μm . The minimum distance between vias on the same layer is 2.5 times the via diameter, and the minimum distance between two consecutive staggered vias is twice the via diameter. The vias must be at least three times their diameter from the substrate edge. Constraints also exist on the catch pads, which are square metallic patches at the extremities of the vias. The catch pads must be at least 50 μm larger than the via diameter.

The rules described here must be followed in the design procedure, to avoid any problems during the fabrication phase.

3. Design of the antenna on a two-layer substrate

First, we will study an antenna to operate in the lower part of the AEHF frequency band (20.2 GHz to 21.2 GHz). As the antenna will be built on LTCC material, the substrate thickness must be a multiple of fired LTCC substrate (0.107 mm). As mentioned in the introduction, the thickness should not be larger than 0.261mm at 20.7 GHz to avoid substantial excitation of surface waves. Thus, the substrate thickness should be no more than two or three LTCC fired layers, 0.214 mm or 0.321 mm.

The optimization of the antenna geometry is carried out with one feed only, to reduce the size of the problem and therefore the computation time. A second feed is added at the end. This approach can be considered if the coupling between the two orthogonal ports is low.

3.1. Characteristics of a single square patch

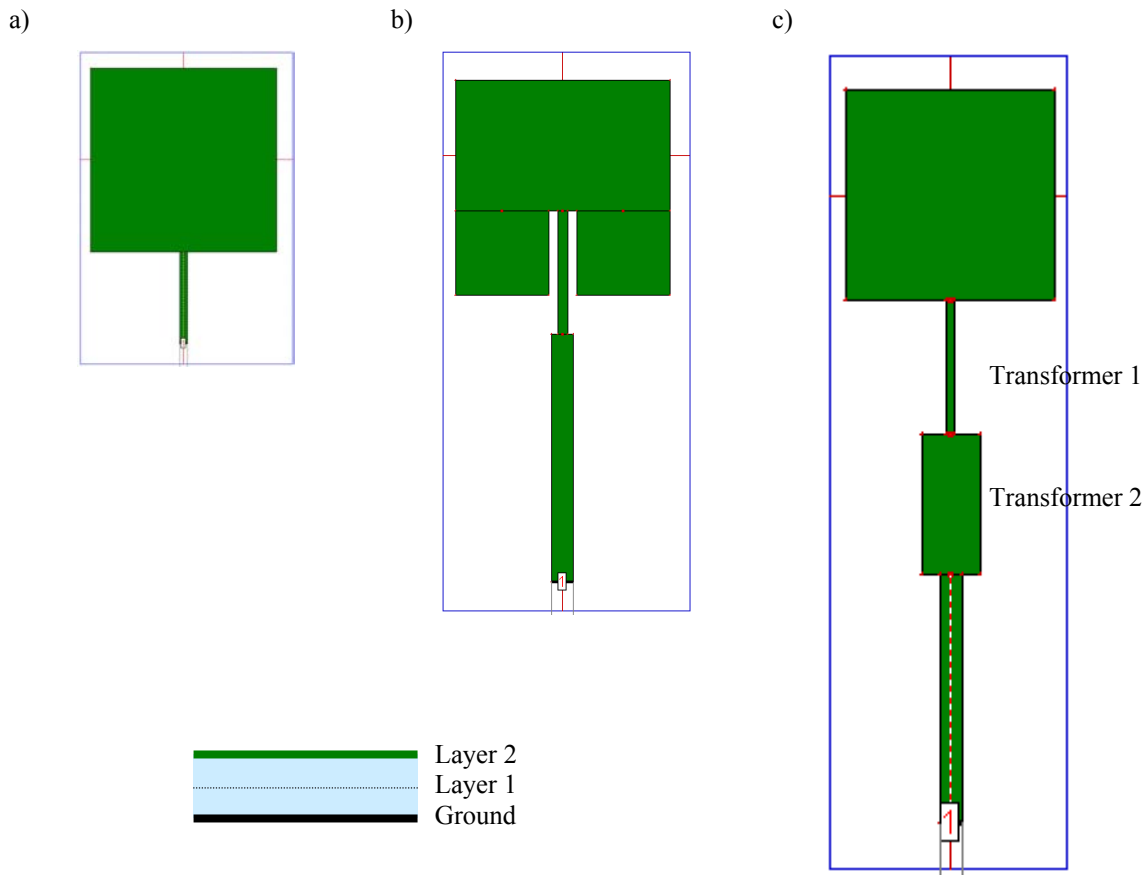


Figure 7. Square patch antenna a) edge fed, b) with inset feed c) edge fed with two quarter-wavelength transformers

The patch dimensions have been evaluated using Sainati's book [11]. A square patch of dimension 2.7 mm resonates at 20.7 GHz. Its impedance at the edge is 468 Ohms. Several solutions exist to match the

input impedance to the conventional 50 Ohms impedance [9] (Figure 7). A simple quarter wavelength transformer can be used. However, its characteristic impedance must be about 153 Ohms, and this impedance is obtained with a microstrip line of width 0.0082 mm. This width is significantly below the minimum line width that can be realised with the LTCC process (see Annex 8.2. , page 32). Another solution involves introducing the feed line in the patch. The impedance of the patch decreases when the feed moves towards the patch centre, and therefore lower input impedance can be considered. A quarter wavelength transformer is still used to achieve the 50 Ohms input impedance, as shown in Figure 7b.

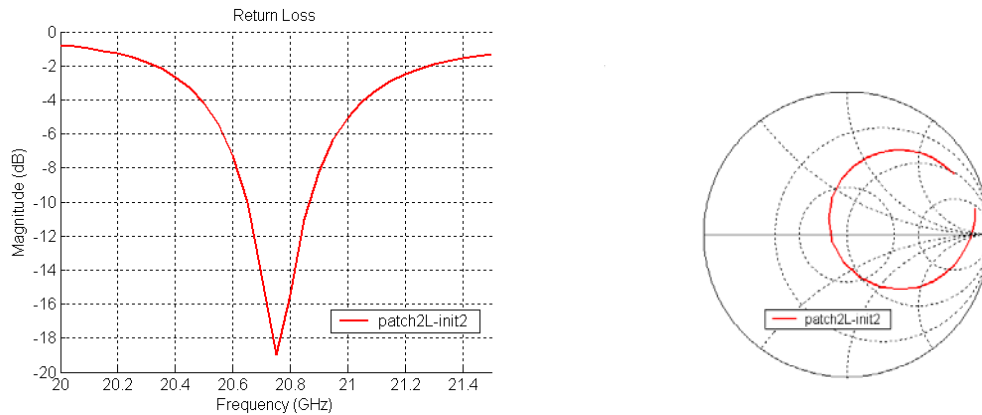


Figure 8. Input impedance of the patch antenna with inset feed

Optimization using IE3D is carried out to find the best feed location. Finally, the best results are obtained with an inset feed 1.06 mm long and with a 0.109 mm air gap. The quarter wavelength transformer is 0.132 mm wide and 1.55 mm long. The input impedance of the patch with an inset feed is shown in Figure 8. As mentioned in the introduction, an impedance bandwidth of 1.06% around 20.76 GHz is obtained (20.65-20.87 GHz).

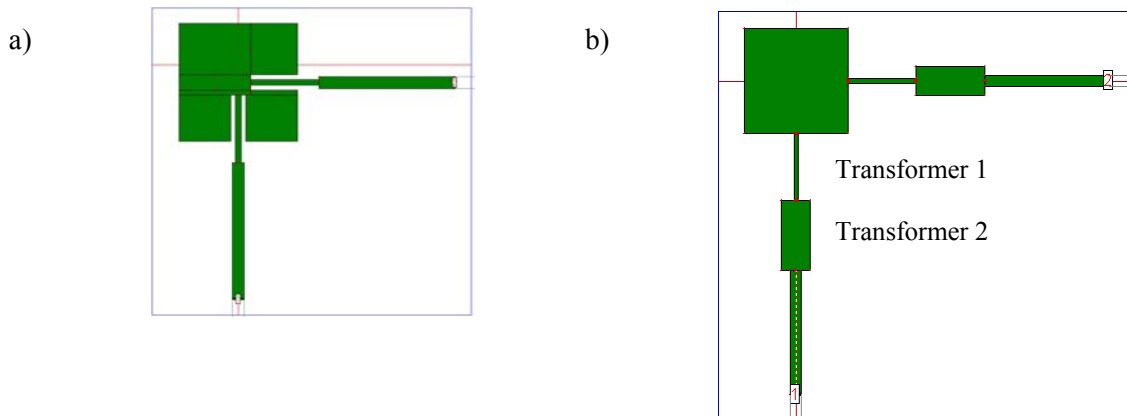


Figure 9. CP configuration of the square patch antenna a) with inset feeds and b) edge fed with two quarter-wavelength transformers

However, the inset feed configuration can not be used for a circularly polarized patch antenna. As shown in Figure 9a, the insertion of a second feed changes the patch geometry and therefore the radiation

mechanism as well. Thus, a solution consisting of a matching circuit composed of two quarter-wavelength transformers is preferred, as shown in Figure 7c for linear polarisation, and in Figure 9b for circular polarisation. The design procedure for the matching circuit is as follows. The minimum possible line width is considered for the first quarter-wavelength transformer. This line of width 0.1 mm has a 79 Ohms characteristic impedance (see Annex 8.2. , page 32). The input impedance becomes 13.1 Ohms after transformation ($79^2 / 468$). Then, the line width of the second quarter-wavelength transformer is calculated to achieve the required 50 Ohms input impedance. The line width of the second quarter-wavelength transformer is 0.72 mm, corresponding to a characteristic impedance of 25.6 Ohms. The lengths of the first and second quarter-wavelength transformers are 1.7 mm and 1.73 mm, respectively. They are different because the propagation constants of these two transmission lines are different, as mentioned in Annex 8.2. , page 32. The patch dimension is 2.6 mm.

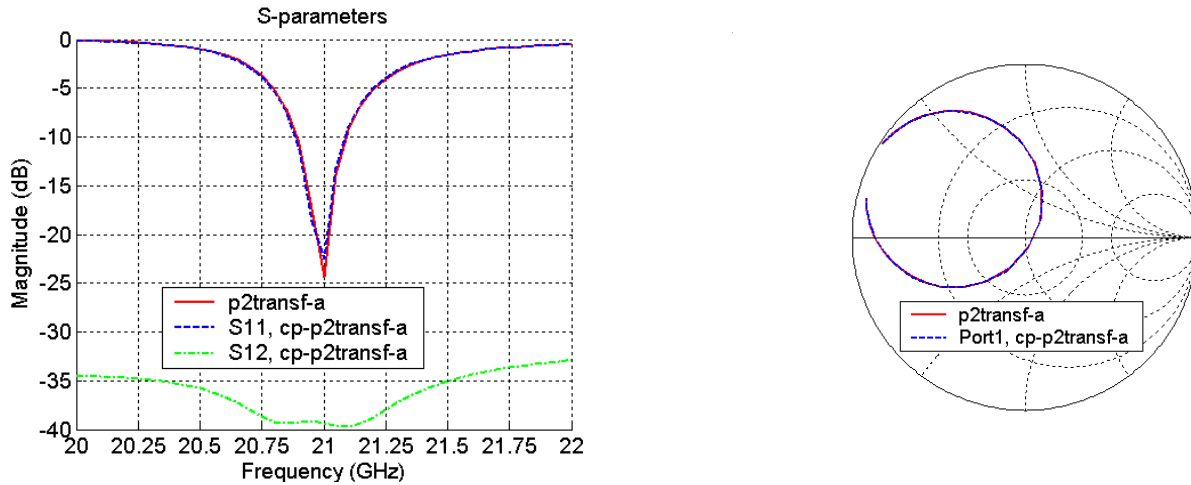


Figure 10. Input impedance of the patch antenna with two quarter-wavelength transformers with one and two ports

The input impedance of the patch with two quarter-wavelength transformers is shown in Figure 10. This figure compares the input impedance of the patch with one and two ports, respectively. As mentioned in the introduction, an impedance bandwidth of about 0.95% around 21 GHz is obtained (~20.9-21.1 GHz) with both configurations. With the two-port configuration, the coupling between the ports is low (less than -39 dB within the impedance bandwidth). This result is obviously not good enough for our application. The technique of stacked resonators is then used to increase the bandwidth. This study is presented in the next sub-section.

3.2. Square patch stacked with a printed ring resonator

The first approach is to add a second patch of the same dimensions as the driven patch on a different layer, and to change the dimensions to optimize the coupling, and therefore to maximize the impedance bandwidth.

In our case, the second patch is placed on the first layer. The driven patch is left on the second layer, to keep more flexibility in terms of impedance characteristics of the microstrip lines (if the driven patch was on the first layer, the line width will be divided by about a factor of two to have the same characteristics impedance as a line printed on layer two).

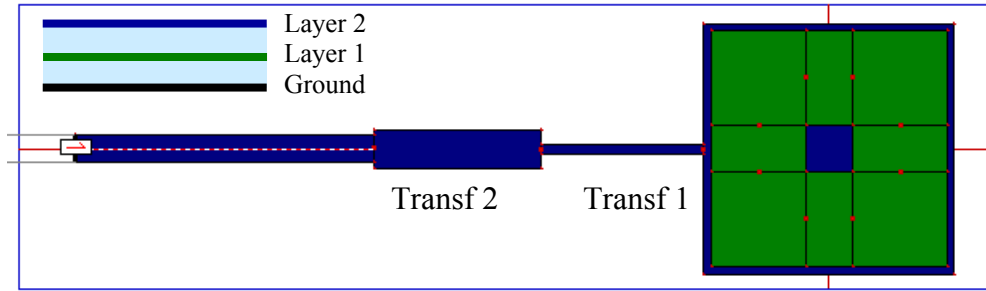


Figure 11. Patch antenna stacked with a square ring resonator

A conventional square patch is then first added on layer one. It appears that the coupling is too strong between the two resonators, and only a dual bandwidth impedance match is obtainable. To reduce the coupling between the resonators, another kind of printed antenna is considered: the ring resonator antenna. Again, the added resonator is on layer one, as shown Figure 11. The ring is centred on the driven patch. The size of the ring is smaller than the size of the patch, as the width of a resonating square ring varies between a quarter wavelength and a half wavelength depending on the ring width, as described in [12]. The dimensions of the ring are optimized to achieve the maximum impedance bandwidth.

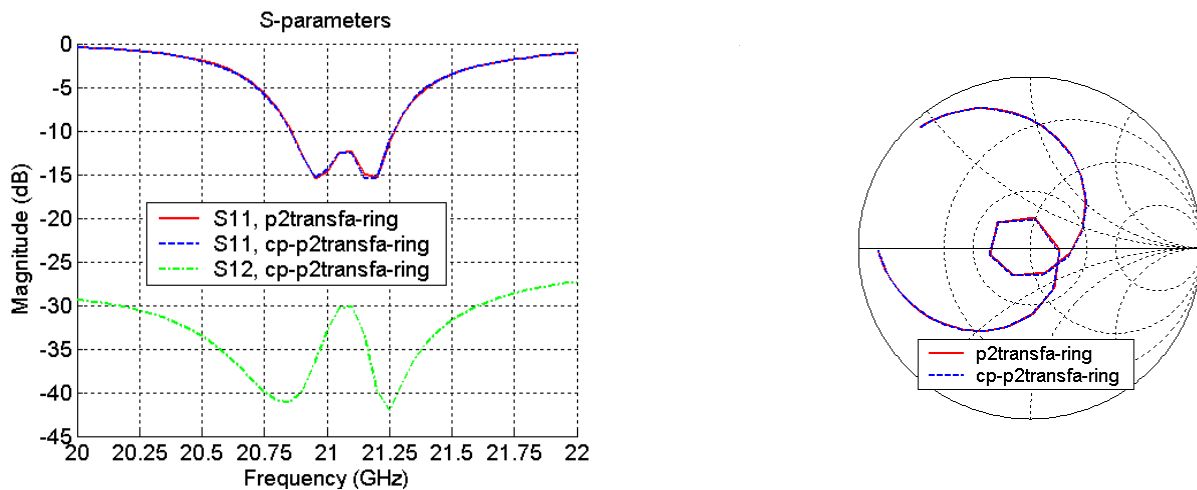


Figure 12. Input impedance of the patch antenna stacked with a square ring resonator

Finally, an impedance bandwidth of 1.9% around $f = 21.05$ GHz is obtained (20.85 GHz to 21.25 GHz). The input impedance is shown in Figure 12 for one and two-port configurations. With the latter, the coupling between the ports is lower than -30 dB within the impedance bandwidth. In the Smith Chart loci, a loop centred on 50 Ohms, representing the coupling between the resonators, is observed. This result is obtained for the following dimensions:

- + Driven patch
 - $W = 2.6 \text{ mm}$
- + Feeding lines
 - Transformer 1: $L_{\text{transf1}} = 1.70 \text{ mm}$, $W_{\text{transf1}} = 0.10 \text{ mm}$
 - Transformer 2: $L_{\text{transf2}} = 1.73 \text{ mm}$, $W_{\text{transf2}} = 0.4 \text{ mm}$
 - $W_{50} = 0.274 \text{ mm}$
- + Ring resonator
 - $W_{\text{in}} = 0.48 \text{ mm}$, $W_{\text{out}} = 2.45 \text{ mm}$

The width of the second transformer is reduced compared to that of a single patch, because the addition of a stacked resonator lowers the input impedance of the antenna. Then, as the quarter-wavelength transformer 1 is kept unchanged, a larger characteristic impedance is required for the second quarter-wavelength transformer, and is obtained with a narrower line width. A 0.4 mm-wide line corresponds to a 39 Ohms characteristic impedance.

Adding the ring antenna doubles the impedance bandwidth, but this is still inadequate for our application. Another technique to enhance the bandwidth is then used. This technique consists of adding other resonators on the same layer [9], [13].

3.3. Patch radiator stacked with a printed ring resonator and parasitic elements

The additional resonators are placed on the first layer. They are directly coupled to the stacked ring. The resonators are two microstrip strips placed symmetrically on both sides of the square ring, parallel to the feeding line. The insertion of the resonators on the top layer, directly coupled to the driven patch, does not improve the impedance bandwidth. The geometry of the antenna with two ports is shown in Figure 13. The procedure to design these parasitic elements is as follows. First, the length of the resonators is chosen to be a half-wavelength. The width is chosen to be narrow to ensure that no orthogonal modes can be excited, and to not increase too much the overall width of the radiating element. Then, an optimization is carried out to obtain the largest possible impedance bandwidth. During this process, the dimensions of the other resonators, the square ring and the driven patch, need to be adjusted to compensate for the additional coupling introduced by the parasitic elements. Finally, the best result in terms of impedance is obtained with the following configuration, according to Figure 13. Again, the addition of the resonators lower the input impedance of the antenna, and the width of the second quarter-wavelength transformer needs to be reduced for impedance compensation.

- | | |
|---------------------------------------------------------------------------------------------------------------------------------------------------------------------------------------------------------------------------------------------------------------------------------------------------------------------------------------------------------------------------------------------------------------------------------------------------------------------------------------------------------------------------------------------------------|----------------------------------------------------------------------------------------------------------------------------------------------------------------------------------------------------------------------------------------------------------------------------------------------------------------------------------------------------------------------------------------------------------------------------------------------------------------|
| <ul style="list-style-type: none"> + Driven patch <ul style="list-style-type: none"> - $W = 2.6 \text{ mm}$ + Feeding lines <ul style="list-style-type: none"> - Transf1: $L_{\text{transf1}} = 1.70 \text{ mm}$, $W_{\text{transf1}} = 0.10 \text{ mm}$ - Transf2: $L_{\text{transf2}} = 1.73 \text{ mm}$, $W_{\text{transf2}} = 0.4 \text{ mm}$ - $W_{50} = 0.274 \text{ mm}$ | <ul style="list-style-type: none"> + Ring resonator <ul style="list-style-type: none"> - $W_{\text{in}} = 0.55 \text{ mm}$, $W_{\text{out}} = 2.45 \text{ mm}$ + Parasitic elements <ul style="list-style-type: none"> - $W_p = 0.5 \text{ mm}$ - $L_p = 2.6 \text{ mm}$ - $s_p = 1.2 \text{ mm}$ |
|---------------------------------------------------------------------------------------------------------------------------------------------------------------------------------------------------------------------------------------------------------------------------------------------------------------------------------------------------------------------------------------------------------------------------------------------------------------------------------------------------------------------------------------------------------|----------------------------------------------------------------------------------------------------------------------------------------------------------------------------------------------------------------------------------------------------------------------------------------------------------------------------------------------------------------------------------------------------------------------------------------------------------------|

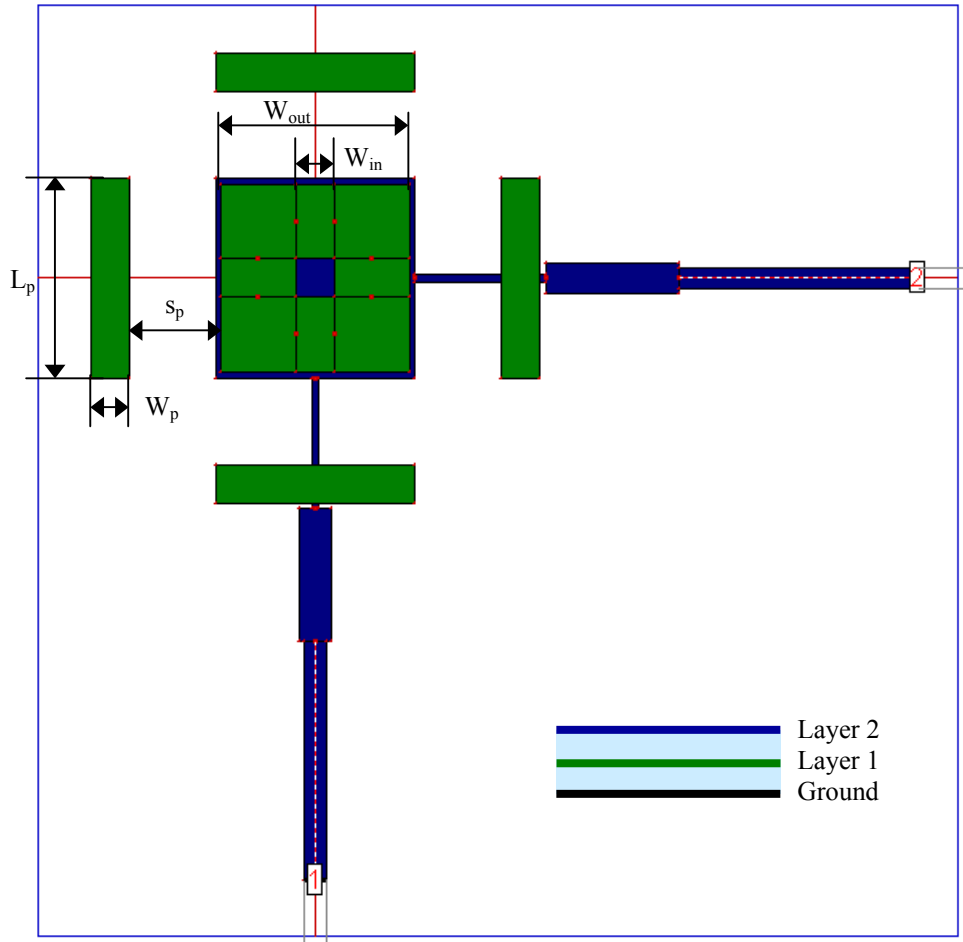


Figure 13. Patch antenna stacked with a ring resonator and coupled to parasitic elements

The input impedance of this antenna is given in Figure 14. The input impedance in the Smith Chart loci makes two loops centred on 50 Ohms impedance. These loops are representative of the coupling between three resonators. The results exhibit an impedance bandwidth of 3.55% around a 21.15 GHz centre frequency (20.77 GHz-21.52 GHz). The coupling between the two ports remains low, and it is lower than -30 dB within the impedance bandwidth.

The addition of a ring resonator improves by a factor of two the impedance bandwidth of a single patch antenna. The use of parasitic resonators on both sides of the ring (four sides for the CP configuration) enhances again the impedance bandwidth by a factor of 3.5 compared to the impedance bandwidth of a single patch. However, the result is still below the specifications for AEHF communications. An attempt has been made to further improve the impedance bandwidth by adding parasitic elements on the second layer, but this was not successful. Another dielectric layer seems necessary to reach our goal of 5% impedance bandwidth. This investigation is presented in the next section.

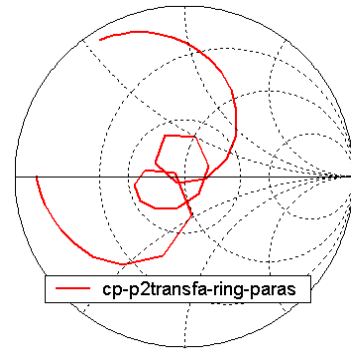
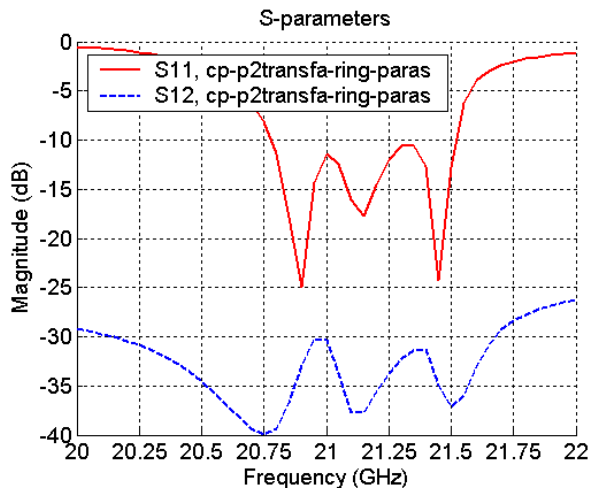


Figure 14. Input impedance of the patch antenna stacked with a ring resonator and coupled to parasitic elements

4. Design of the antenna on a three-layer substrate

4.1. Preliminary investigations

The first steps in the investigation of bandwidth enhancement of a square patch antenna on a three-layer LTCC substrate are exactly the same as the ones followed in the study of bandwidth improvement of the patch on a two-layer LTCC substrate. Two configurations can be considered: the driven patch is placed on the second layer and therefore it is overlapped by the third layer or, the driven patch is put on the top layer, and all the additional resonators are introduced underneath. The latter is chosen, as it gives more flexibility in terms of transmission line impedance, as mentioned in section 3.2. . In this sub-section, the results from a single square patch to a square patch stacked with a square ring coupled to parasitic elements are presented, with one and two ports.

4.1.1. Antennas with one port

Using Sainati's book [11], the dimensions and the input impedance of a single square patch are estimated. A square patch of size 2.61 mm resonates at 20.7 GHz, and has an input impedance of 510 Ohms. Two transformers are cascaded to obtain a 50 Ohms input impedance. The dimensions are given in Annex 8.4. and the corresponding characteristic impedance can be found in Annex 8.2. .

The single patch printed on a three-layer substrate exhibits a 1.26% impedance bandwidth around a centre frequency of 20.55 GHz (20.42 GHz to 20.68 GHz). A slight bandwidth improvement is obtained compared to a patch on a two-layer substrate. The input impedance is given in Figure 15. The addition of a stacked ring on layer 2 (0.214 mm above the ground) improves the impedance bandwidth (1.94% around 20.6 GHz or 20.4 GHz to 20.8 GHz). As shown in Figure 15, the ring resonator increases the bandwidth in the higher frequencies. When the parasitic elements are introduced in the structure on both side of the square ring, the impedance bandwidth increases to 4.15% around the 20.73 GHz centre frequency. Due to the coupling between resonators, the patch resonance is shifted down. The parasitic elements resonate in the upper part of the bandwidth, and thus increase the bandwidth in the higher frequency.

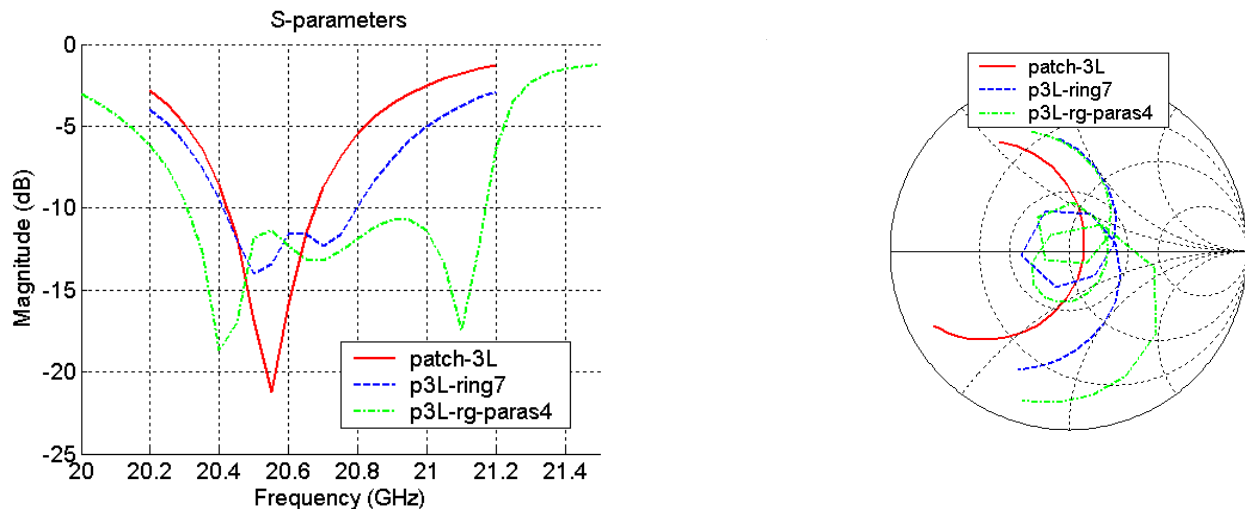


Figure 15. Input impedance of the single patch, the patch stacked with a ring, and a patch stacked with a ring coupled to parasitic elements, fed by a single port

In the single port configuration, the impedance bandwidth of the antenna is improved. The next subsection presents the results of the antennas with two ports.

4.1.2. Antennas with two ports

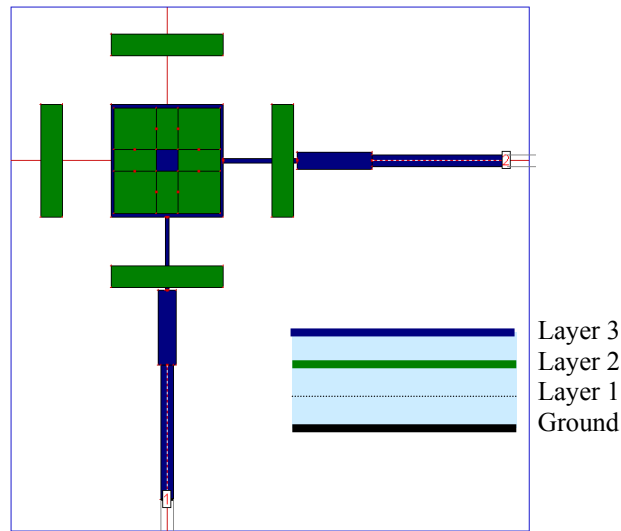


Figure 16. Two-port patch antenna stacked with a ring resonator and coupled to parasitic elements on a three-layer substrate

The insertion of a second port, needed to generate the circular polarisation, slightly modifies the input impedance. The dimensions of some resonators are then changed to retain the same bandwidth. Figure 17 gives the input impedance of the patch stacked with a ring and a patch stacked with a ring coupled to parasitic elements, in the two-port configuration. The dimensions of these antennas are reported in Annex 8.4. . The antenna composed of the patch and the stacked ring exhibits a slightly larger bandwidth than the same antenna with one port (2.19% around 20.575 GHz – 20.35 to 20.8GHz - against 1.94%), whereas the other antenna has a slightly narrower impedance bandwidth (4.08% around 20.825 GHz – 20.4 to 21.25 GHz – against 4.15%). Figure 17 also shows that the coupling between the ports increases a little bit when the parasitic elements are inserted. However, the coupling stays below –25 dB in most of the frequency band.

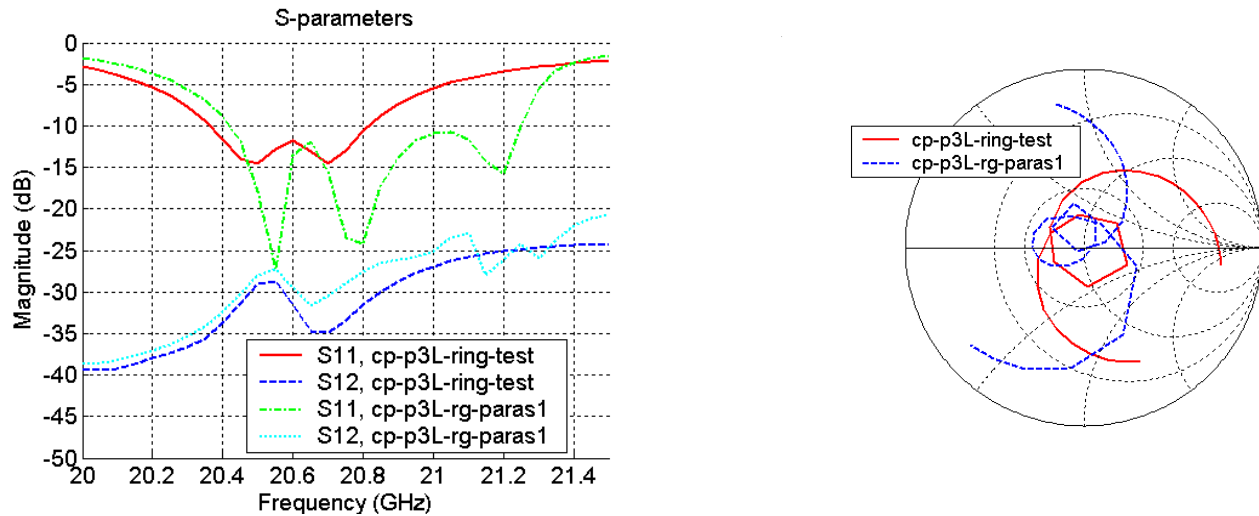


Figure 17. Input impedance of the patch stacked with a ring, and a patch stacked with a ring coupled to parasitic elements, fed by two ports

The obtained impedance bandwidth is larger than the one obtained with the same number of resonators but on a two-layer substrate (4.08% against 3.55%). However, the result is not sufficient regarding the specification of AEHF communication systems. The addition of a layer gives another degree of freedom. Other resonators can be inserted to further increase the bandwidth. A solution is proposed in the next-sub section.

4.2. The final radiating element

Another resonator is finally added on the first layer. This resonator is a square ring resonator, whose dimensions are optimized to further increase the impedance bandwidth. Again, the dimensions of the other resonating elements are modified to counteract the coupling introduced by this new element. The geometry of the radiating element is shown in Figure 18, and its dimensions are given in Annex 8.4. . Note that the transformer dimensions are changed compared to the previous case (now $W_{\text{transf}} = 0.1$ mm and $L_{\text{transf}} = 1.9$ mm).

Finally, an impedance bandwidth larger than 5% is obtained with the help of the second ring placed on the first layer. Its contribution is in the lower part of the frequency band. The input impedance is indicated in Figure 19. The impedance bandwidth reaches 5.31% around a 20.71 GHz centre frequency (20.16 GHz to 21.26 GHz). The coupling between the two ports is lower than -25 dB throughout the bandwidth. The appearance of a third loop is visible in the Smith Chart loci.

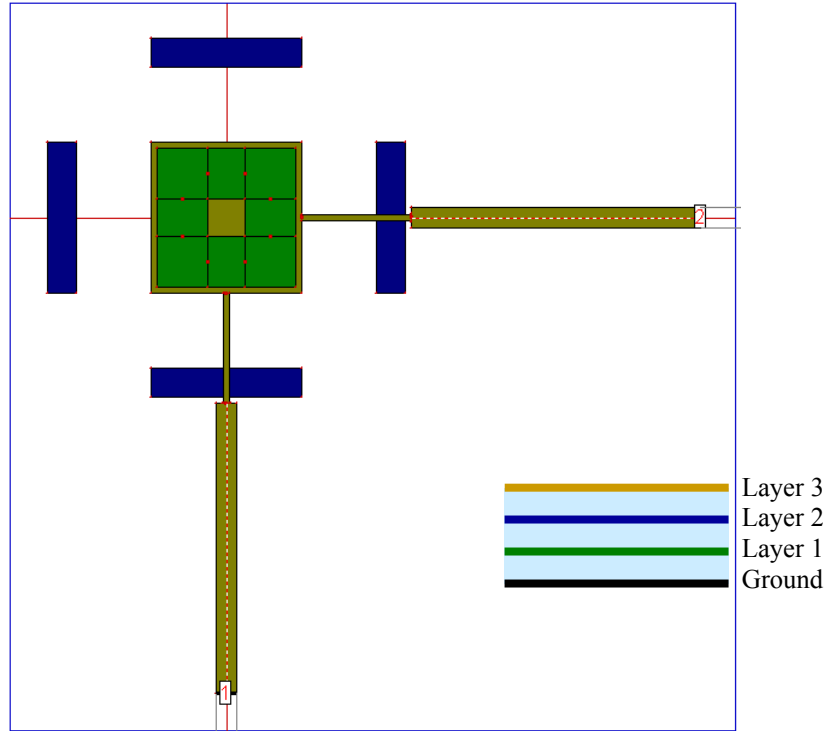


Figure 18. Two-port patch antenna stacked with two ring resonators and coupled to parasitic elements

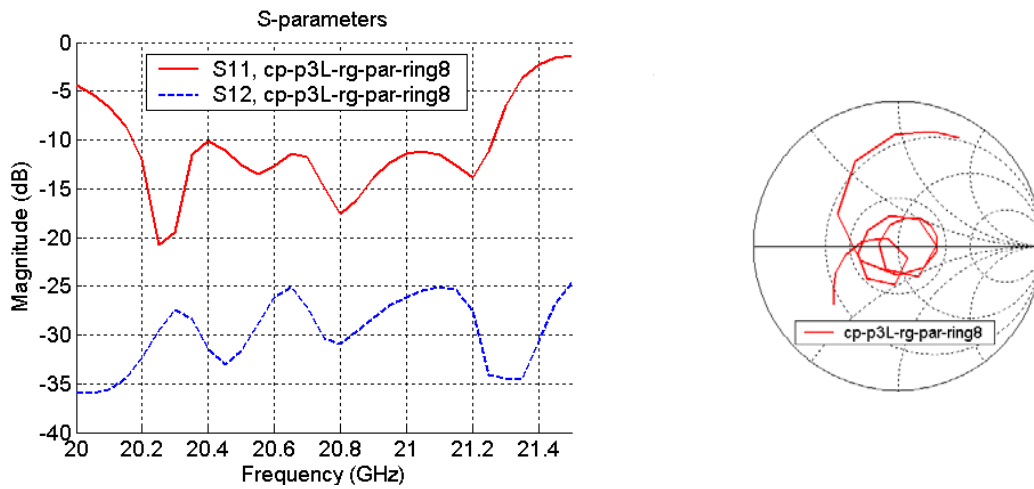


Figure 19. Input impedance of the two-port patch antenna stacked with two ring resonators and coupled to parasitic elements

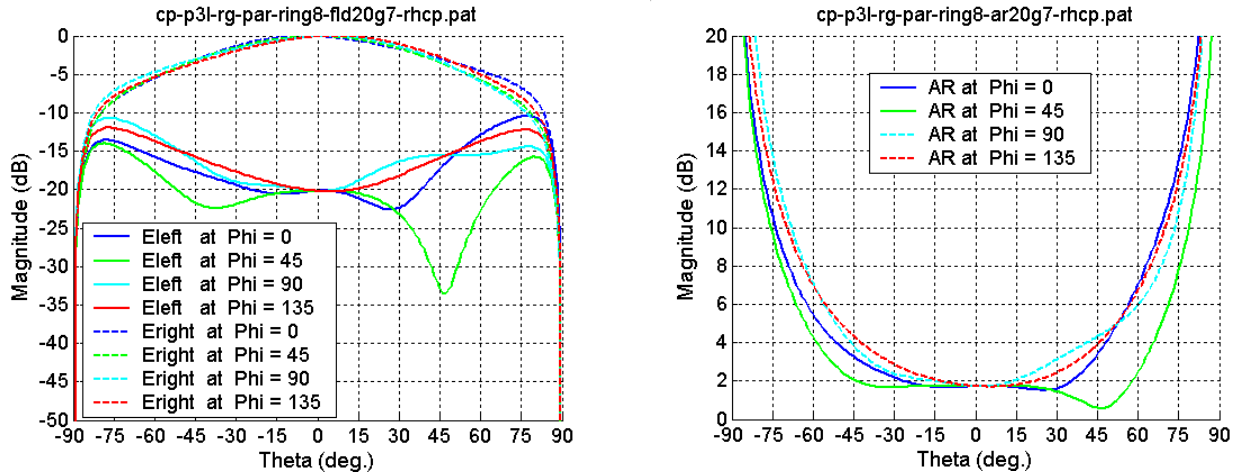


Figure 20. Radiation patterns in circular polarisation and axial ratio of the two-port patch antenna stacked with two ring resonators and coupled to parasitic elements

The radiation patterns in circular polarisation and the corresponding axial ratios are shown for different planes at 20.7 GHz in Figure 20. The radiation characteristics are summarized in Table 1. The main beams are slightly titled ($\pm 4^\circ$) due to the radiation of the feed lines. The half-power beamwidth is about 90° in all the planes. The power level at $\pm 60^\circ$ is about 5 to 6 dB below the maximum radiated power. The half-power axial ratio varies significantly from one plane to another, and it is minimum in the 45° plane and maximum in the 135° planes. The axial ratio at $\pm 60^\circ$ is lower than 7.0 dB, except in the 45° plane where it is lower than 4.5 dB.

Table 1 : Summary of the radiation characteristics of the two-port patch antenna stacked with two ring resonators and coupled to parasitic elements

Plane	$\varphi = 0^\circ$	$\varphi = 45^\circ$	$\varphi = 90^\circ$	$\varphi = 135^\circ$
HPBW (deg.)	91	88	90	88
Power Level at -60° (dB)	-5.4	-5.2	-4.6	-5.3
Power Level at $+60^\circ$ (dB)	-4.5	-5.7	-5.9	-5.0
3dB Axial Ratio (deg.)	85 [-42; 43]	115 [-53; 62]	66 [-38; 28]	69 [-32; 37]
AR at -60° (dB)	5.5	4.3	7.1	7.0
AR at 60° (dB)	7.0	2.5	6.0	6.7

These radiation characteristics are obtained when the two ports are directly fed with a 90° phase difference to generate the circular polarisation. A feeding circuit needs to be designed to feed the antenna. Its influence should be taken into account in the evaluation of the radiation characteristics. The design of the feeding circuit is described in the next sub-section.

4.3. The feeding system

The feeding system is built following several steps. The final design of the antenna with the feeding system is shown in Figure 21. All the antenna dimensions, including the feeding system, are indicated in Annex 8.4. .

First, the transformers need to be bent. Their length and width are adjusted to maintain the impedance bandwidth. A line with a width of 0.15 mm and a mean length of 0.515 mm is the optimum design. The input impedance is indicated in Figure 22 (elt1-single2). Then, the T-junction is designed with 50 Ohms lines. The bends are taken into account to achieve the 90 deg. phase difference between the two output ports. The length and width of the last transformer are adjusted for impedance bandwidth performance. Finally, for the dimensions given in Annex 8.4. , a phase difference of 90.2° is obtained. Note that the magnitudes of the transmission factors S21 and S31 (between input 1 and outputs 2 and 3) are not equal (-3.9 dB and -2.6 dB, respectively).

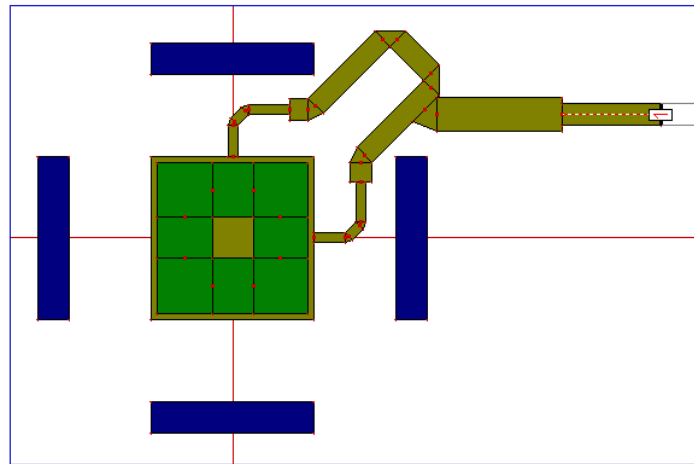


Figure 21. Circularly polarized multi-resonators antenna

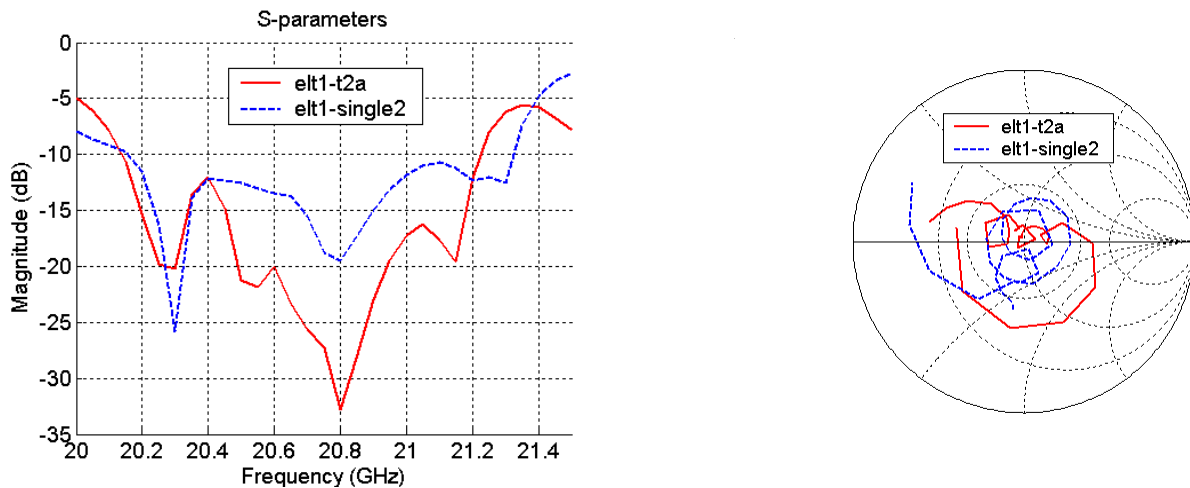
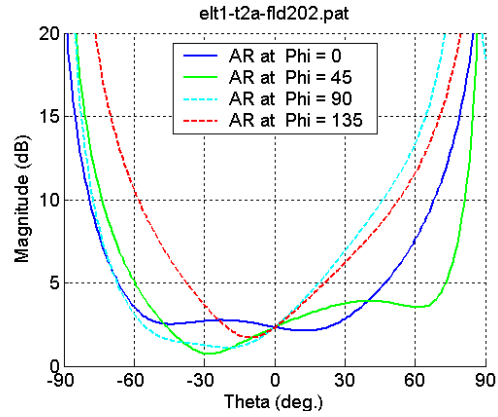
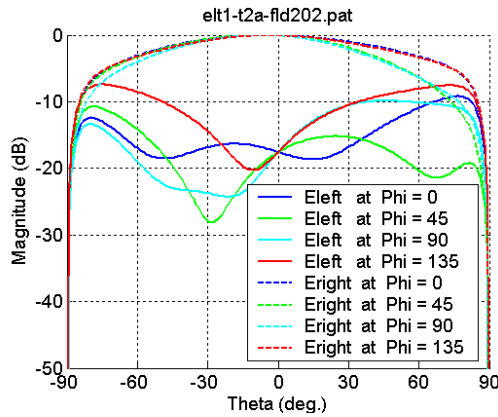


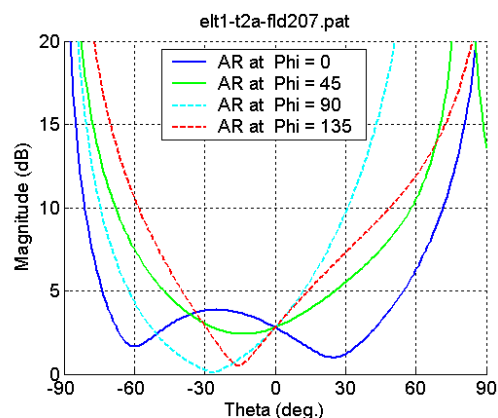
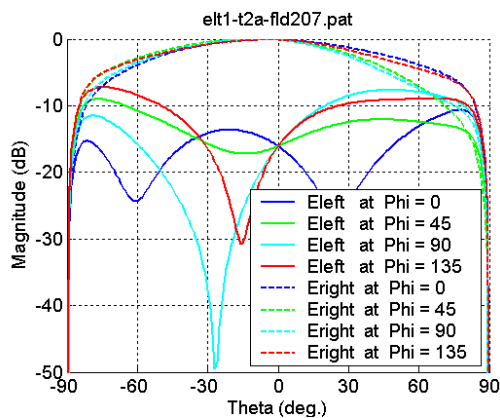
Figure 22. Input impedance of the final antenna with and without its feeding circuit

The input impedance of the final antenna with its feeding circuit is shown in Figure 22 (elt1-t2a). An impedance bandwidth of 5.08% centred on 20.675 GHz (21.15 GHz to 21.2 GHz) is obtained. This bandwidth is slightly narrower than the impedance bandwidth of the antenna without a feeding circuit.

f = 20.2 GHz



f = 20.7 GHz



f = 21.2 GHz

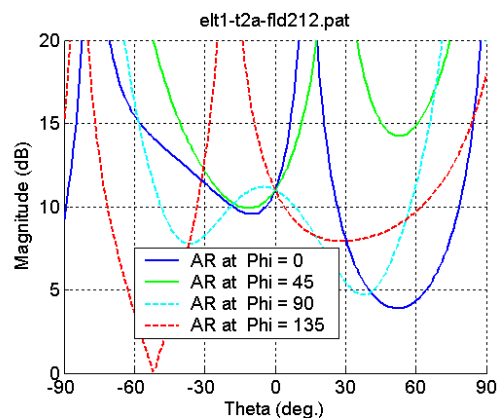
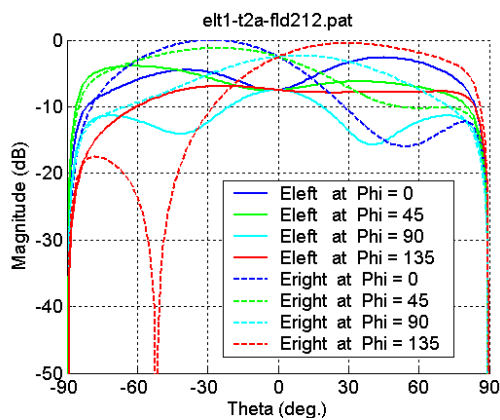


Figure 23. Radiation patterns and axial ratios of the antenna with its feeding circuit

The radiation patterns and the axial ratios of the antenna with its feeding circuit are shown in Figure 23 in the main planes ($\phi = 0^\circ, 45^\circ, 90^\circ$ and 135°) for three different frequencies. The radiation patterns at $f = 21.2$ GHz does not represent the conventional radiation pattern of a printed antenna. The contribution of the feeding system is important, and significantly deteriorates the radiation characteristics. This can be seen especially with the representation of the axial ratio. Note that the feeding circuit is not feeding the ports with exactly the same magnitude and a phase difference of 90° , contributes also to the degradation of the radiation performances.

Table 2 : Summary of the radiation characteristics of the antenna with its feeding system at 20.7 GHz

Plane	$\phi = 0^\circ$	$\phi = 45^\circ$	$\phi = 90^\circ$	$\phi = 135^\circ$
HPBW (deg.)	110	99	91	107
Power Level at -60° (dB)	-3.7	-2.9	-3.5	-3.0
Power Level at $+60^\circ$ (dB)	-3.7	-7.1	-7.4	-4.4
3dB Axial Ratio (deg.)	89 [-45; 44]	32 [-29; 3]	55 [-54; 1]	31 [-30; 1]
AR at -60° (dB)	1.6	7.5	4.3	10.6
AR at 60° (dB)	6.3	10.5	30.0	11.9

5. Arrays of four radiating elements

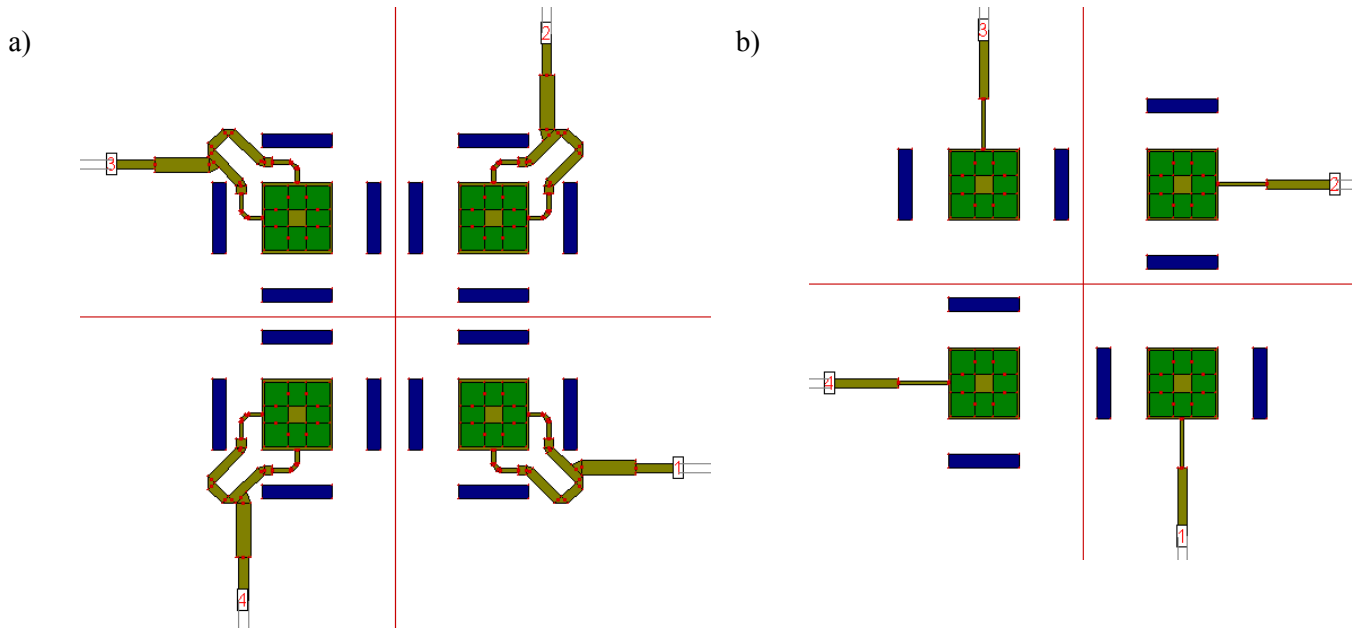


Figure 24. Array with a) four circularly polarized antennas and b) four linearly polarized antennas

The element developed in the previous section is used in an array configuration. As its axial ratio is not so good, the elements are rotated and fed with a 90° phase shift with respect to each other. The sequential rotation of the elements along with sequential phase shift feeding, improves the axial ratio. This technique was first developed to obtain a circularly polarized array with linearly polarized elements [14],[15], but this concept has since been used with circularly polarized elements. Figure 24a shows the circularly polarized four element array, while Figure 24b presents the circularly polarized array realised with four linearly polarized (LP) radiating elements. The resonators of the CP and LP elements have the same dimensions. The only difference is the dimensions of the transformer of the LP element ($W_{\text{transfl}} = 0.12 \text{ m}$, $L_{\text{transfl}} = 1.80 \text{ mm}$), which are adjusted for impedance bandwidth purposes. Note that the CP elements generate left-hand circular polarisation (LHCP), whereas the CP elements described in the previous section generate right-hand circular polarisation (RHCP). Only the feeding system needs to be reversed to switch from LHCP to RHCP.

The radiation patterns of the arrays of four CP and LP radiating elements are shown in Figure 25 in the main planes ($\varphi = 0^\circ, 45^\circ, 90^\circ$ and 135°) for three different frequencies. The main difference between the patterns generated by the two different arrays is the level of cross-polarisation. It is much higher with the LP radiating elements. For the two arrays, one can observe that the pattern in the $\varphi = 0^\circ$ plane is identical to the pattern in the $\varphi = 90^\circ$ plane, and the pattern in the $\varphi = 45^\circ$ plane is identical to the pattern in the $\varphi = 135^\circ$ plane. The half-power beamwidths are similar in all planes. The cross-polarisation level is null in the boresight direction in all planes and for all frequencies. With the array of CP elements, its level increases with frequency, and reaches a maximum of -10 dB in the $\varphi = 0^\circ$ and $\varphi = 90^\circ$ planes and -6.5 dB in the $\varphi = 45^\circ$ and $\varphi = 135^\circ$ planes. Note that the four patterns are similar in the four planes at $f = 20.2 \text{ GHz}$. At $f = 21.2 \text{ GHz}$, some side lobes appear in the planes, representative of the array configuration. With the array of LP elements, the level of cross-polarisation becomes higher than the level of co-polarisation in the $\varphi = 45^\circ$ and $\varphi = 135^\circ$ planes and for all the frequencies from $\theta = 45^\circ$. In these

planes, the maximum cross-polarisation level fluctuates between -10 dB and 5 dB. High-level shoulders appears in the $\varphi = 45^\circ$ and $\varphi = 135^\circ$ planes for all the frequencies. Note that the half-power beamwidths obtained with this array is of the same order as the HPBW obtained with the array of CP elements. The axial ratios (ARs) of the arrays of four CP and LP radiating elements shown in Figure 26 in the main planes ($\varphi = 0^\circ, 45^\circ, 90^\circ$ and 135°) for three different frequencies. One can first notice that an axial ratio of 0 dB is achieved in the boresight direction for all the frequencies. This is due to the sequential rotation operated on the elements. As the radiation patterns are identical in the $\varphi = 0^\circ$ and $\varphi = 90^\circ$ planes, and in the $\varphi = 45^\circ$ and $\varphi = 135^\circ$ planes as well, the axial ratios are similar in the same planes. Their 3 dB bandwidth is larger in the $\varphi = 0^\circ$ and $\varphi = 90^\circ$ planes than in the $\varphi = 45^\circ$ and $\varphi = 135^\circ$ planes. For the array of CP elements, the axial ratios are better at low frequency, and their 3 dB bandwidths decrease when the frequency increases. At 20.2 GHz, the 3 dB AR bandwidth is double in the $\varphi = 0^\circ$ and $\varphi = 90^\circ$ planes compared to the 3 dB AR bandwidth in the $\varphi = 45^\circ$ and $\varphi = 135^\circ$ planes (142° against 72°). The 3 dB AR bandwidth decreases to about 35° in all the planes at 21.2 GHz. For the array of LP elements, the 3 dB axial ratio bandwidths are narrower, at 20.2 GHz and 20.7 GHz, than the ones obtained with the previous array. At the frequency of 21.2 GHz, they are of the same order in the $\varphi = 45^\circ$ and $\varphi = 135^\circ$ planes (38° compared to 31°), and larger in the $\varphi = 0^\circ$ and $\varphi = 90^\circ$ planes (80° against 38°). The radiation characteristics for the array of CP elements are summarised at 20.2 GHz and 20.7 GHz in Table 3 and Table 4, respectively. The radiation characteristics for the array of LP elements are summarised at 20.7 GHz in Table 5.

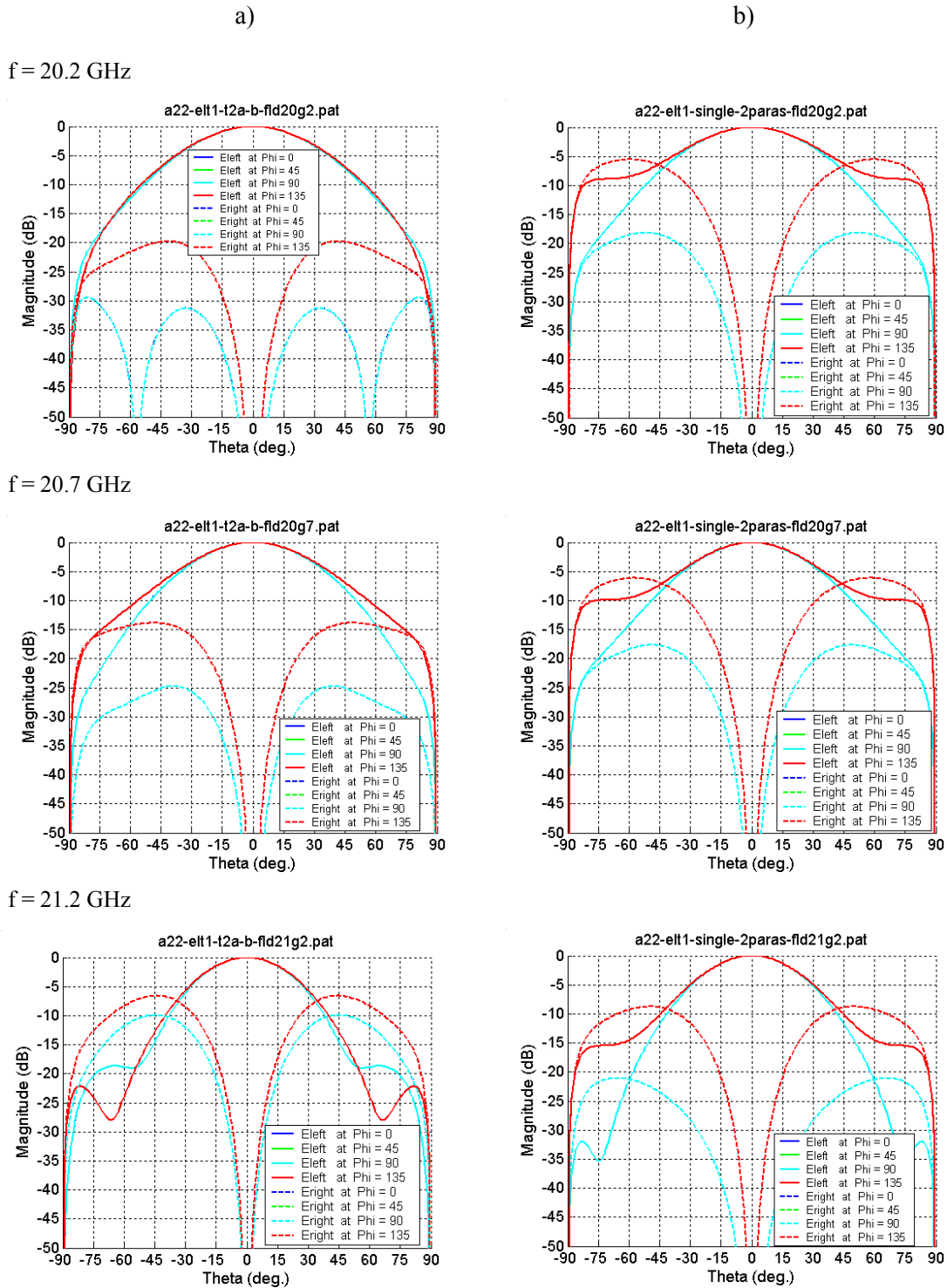


Figure 25. Radiation patterns of the arrays with a) CP radiating elements and b) LP radiating elements

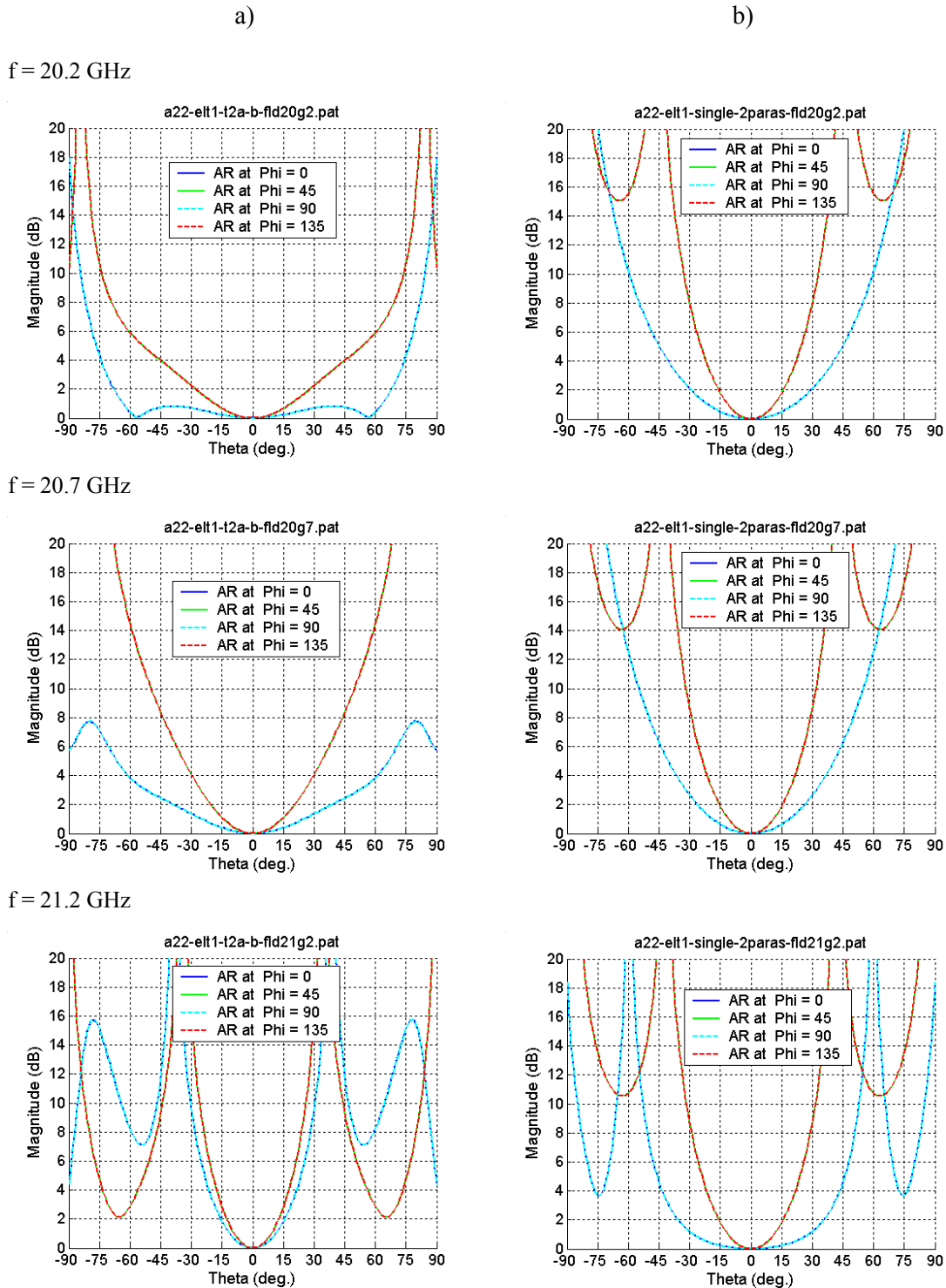


Figure 26. Axial Ratios of the arrays with a) CP radiating elements and b) LP radiating elements

Table 3 : Summary of the radiation characteristics of the array of four circularly polarized radiating elements at 20.2 GHz

Plane	$\varphi = 0^\circ$	$\varphi = 45^\circ$	$\varphi = 90^\circ$	$\varphi = 135^\circ$
HPBW (deg.)	58	60	58	60
3dB Axial Ratio (deg.)	142 [-71; 71]	72 [-36; 36]	142 [-71; 71]	72 [-36; 36]
AR at -60° (dB)	0.43	5.9	0.43	5.9
AR at 60° (dB)	0.43	5.9	0.43	5.9

Table 4 : Summary of the radiation characteristics of the array of four circularly polarized radiating elements at 20.7 GHz

Plane	$\varphi = 0^\circ$	$\varphi = 45^\circ$	$\varphi = 90^\circ$	$\varphi = 135^\circ$
HPBW (deg.)	56	58	56	58
3dB Axial Ratio (deg.)	104 [-52; 52]	50 [-25; 25]	104 [-52; 52]	50 [-25; 25]
AR at -60° (dB)	3.85	14.5	3.85	14.5
AR at 60° (dB)	3.85	14.5	3.85	14.5

Table 5 : Summary of the radiation characteristics of the array of four linearly polarized radiating elements at 20.7 GHz

Plane	$\varphi = 0^\circ$	$\varphi = 45^\circ$	$\varphi = 90^\circ$	$\varphi = 135^\circ$
HPBW (deg.)	52	54	52	54
3dB Axial Ratio (deg.)	64 [-32; 32]	38 [-19; 19]	64 [-32; 32]	38 [-19; 19]
AR at -60° (dB)	12.5	14.3	12.5	14.3
AR at 60° (dB)	12.5	14.3	12.5	14.3

6. Concluding remarks

A circularly polarized antenna realised in printed technology has been studied. This antenna has been designed considering constraints imposed by the packaging technology (LTCC), and by the application (an array for Advanced EHF communications). The impedance bandwidth of a conventional square patch antenna has been improved from 1% to 3.5% when a 0.214 mm thick substrate is considered, and to 5.1% when a 0.321 mm thick substrate is used. The bandwidth enhancement technique used is based on the addition of resonators on different layers coupled to the driven patch. The radiation characteristics of the radiating element are relatively good in the lower and centre parts of the bandwidth in terms of half-power beamwidth, and axial ratio as well, but they are significantly below the requirements in the upper part of the frequency band. This is mainly due to the unwanted contribution of the radiation of the microstrip feeding circuit.

Two arrays of four elements have also been investigated. The results in terms of radiation characteristics of an array of four circularly polarized (CP) elements are compared to the results of an array of four linearly polarized elements arranged in a sequential rotation to obtain the circular polarization. The array with CP elements exhibits better performance, especially in terms of axial ratio.

However, the results are not constant throughout the bandwidth. Another radiating element should be developed with a design suitable for an array for AEHF communications. In particular, the radiation from the feeding system, required to generate the circular polarization, must be minimized to avoid interference with the antenna radiation. A solution using the aperture-coupled technique can be applied to achieve this goal. The radiating element can also be designed in a cavity to reduce or suppress the coupling between elements in an array configuration.

7. References

- [1] B. Geller, B. Thaller, A. Fathy, M. J. Liberatore, H. D. Chen, G. Ayers, V. Pendrick and Y. Narayan, "LTCC-M: an Enabling Technology for High Performance Multilayer RF Systems", *Microwave Journal*, Vol. 42, No. 7, July 1999, pp 64-72.
- [2] D. Sturzebecher, J. Leen, R. Cadotte, J. DeMarco, T.-D. Ni, T. Higgins, M. Popick, M. Cummings, B. VanMeerbeke, T. Provencher, B. Kimble, K. Shalkhauser, R. Simons, "20 GHz LTCC Phased Array Module", *IEEE MTT international Symposium*, 1996, Vol. 2, pp 991-994.
- [3] DuPont Microcircuit Materials, "DuPont Green Tape Design and Layout Guideline, 1998, www.DuPont.com/mcm.
- [4] Ferro Electronic Materials, <http://www.ferro.com>.
- [5] Heraeus, Circuit Material Division, <http://www.4cmd.com/circuitmaterials>.
- [6] Northrop Grumman, Advanced Ceramics Facility, <http://sensor.northgrum.com/esss/ltcc/ltcc.htm>
- [7] Electro-Science Laboratories, <http://electroscience.com>.
- [8] J. A. Kinzel, B. J. Edward and D. Rees, "V-band, Spaced-Based Phased Arrays", *Microwave Journal*, Jan. 1987, pp 89-102.
- [9] R. Garg, P. Bhartia, I. Bahl and A. Ittipiboon, "Microstrip Antenna Design Handbook", Artech House, 2001.
- [10] VTT Electronics, Finland, <http://www.vtt.fi>
- [11] R. A. Sainati, "CAD of Microstrip Antennas for Wireless Applications", Artech House, 1996.
- [12] P. Moosavi Bafrooei and L. Shafai, "Characteristics of Single- and Double-Layer Microstrip Square-Ring Antennas, *IEEE Trans. On Ant. and Prop.*, Vol. 47, No 10, October 1999, pp 1633-1639.
- [13] M. Clénet and L. Shafai, "Comparison of Wideband Single Layer Microstrip Array Antennas for LMCS/LMDS Applications", AP-2000, Davos, Switzerland, p143.
- [14] J. Huang, "A technique for an array to generate circular polarization with linearly polarized elements", *IEEE Transactions on Antennas and Propagation*, Volume: 34 Issue: 9, September 1986, pp 1113 –1124.
- [15] P.S. Hall, J. S. Dahele and J. R. James, "Design principles of sequentially fed, wide bandwidth, circularly polarized microstrip antennas", *IEE Proceedings-Microwaves, Antennas and Propagation Proceedings Part. H*, Volume 136, Issue 5, Oct. 1989, pp 381 – 389.

8. Annexes

8.1. Annex 1: LTCC technology

Table 6 : LTCC Manufacturers and Process Characteristics

Manufacturers	Nationality	Processes					
		DuPont 951	DuPont 943	Ferro A6	Heraeus CT700	Heraeus CT2000	Sarnoff
VTT	FI	X	X	x			
IMST	DE	X					
Thales Microwave	FR	X	x	X	x	x	
Via-Electronic	DE	X					
National Semiconductor	USA	X	X	X			
C-MAC - Scrantom	CA-USA ¹	X	X	X	X	X	
Dielectric Laboratories	USA						X*

X: manufacturing, x: prototyping, X*: LTCC-M

¹ LTCC facilities belong to Scrantom, a company based in California. Scrantom is owned by C-Mac, whose headquarter is in Montreal.

Table 7 : Process Characteristics

	VTT	IMST	National Semiconductor	C-MAC Scantom	Via-Electronic	Thales
Line width/spacing	200 (100 for prototyping)	130	50	75	100 /50	125
Width tolerance				+/- 12.5		+/- 25
Via diameter	150	150	90	100	100	125
Via pad	250	150-300	132	150	150	150
Min. thickness	4 layers	2-4 layers	2-4 layers	3 layers	100	
Max thickness		unlimited			2.3 mm	24 layers
Max. part size	4.5"x4.5"	3.5"x3.5"	5"x5"	6"x6"	6.8"x6.8"	4.5"x4.5"
Resistor tolerances (on Top/buried)	N/A	?	+/- 30% (1% trimmed)/ +/- 30%	10% to 50% (buried)	1% trimmed (on top)	+/- 30% (5% trimmed)/ +/- 50%
Capacitor tolerance	N/A		(+/-) 20% special tape	10% special tape	A	
Inductor	N/A			A		
Ball Grid Array			A		A	A

Dimensions are in microns unless specified. A: Available, N/A: Non Available.

8.2. Annex 2: Microstrip line impedance versus substrate thickness and line width

8.2.1. $h = 0.214$ mm (two LTCC layers)

Table 8 : Characteristics impedance versus line width for a two-layer LTCC substrate

Impedance (Ohms)	Line width (mm)	Guide wavelength (mm) (at $F = 20.7$ GHz)	Effective dielectric permittivity
25.6	0.720	6.92	5.80
39.0	0.4	6.23	5.40
50	0.274	6.35	5.19
70.71	0.132	6.55	4.88
79	0.010	6.61	4.79
98	0.050	6.72	4.65
153	0.008	6.81	4.52

8.2.2. $h = 0.321$ mm (three LTCC layers)

Table 9 : Characteristics impedance versus line width for a three-layer LTCC substrate

Impedance (Ohms)	Line width (mm)	Guide wavelength (mm) (at $F = 20.7$ GHz)	Effective dielectric permittivity
27.5	0.75	5.98	5.85
35.35	0.624	6.06	5.69
50	0.35	6.283	5.31
75.6	0.15	6.52	4.92
88	0.1	6.60	4.81

8.3. Annex 3: impedance bandwidth enhancement of a patch with an inset feed

The technique to improve the impedance bandwidth of a printed antenna has also been applied to a patch with an inset fed. That investigation is reported in this Annex.

8.3.1. Patch with an inset feed stacked with a square ring

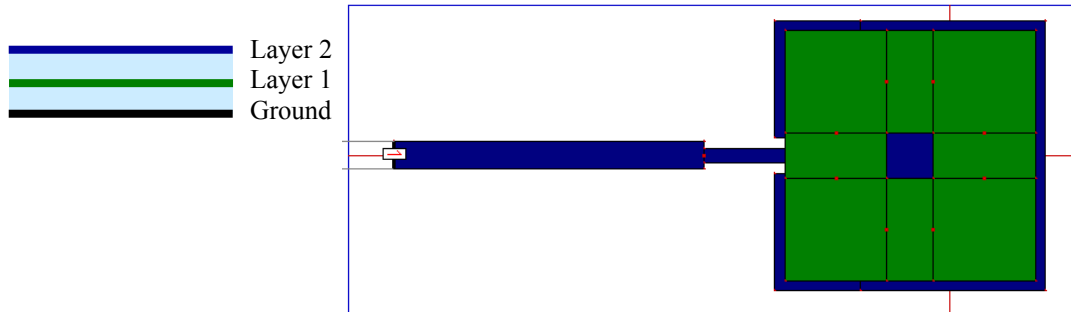


Figure 27. Patch antenna stacked with a square ring resonator

Figure 27 shows the geometry of the radiating element. The ring, placed on the first layer, is centred on the driven patch. The size of the ring is smaller than the size of the patch, as the width of the ring varies between a quarter of guided wavelength and a half guided wavelength depending on the ring width, as described in [12]. The dimensions of the ring are optimized to achieve the maximum impedance bandwidth. Finally, an impedance bandwidth of 2.16% around $F = 2.084$ GHz is obtained (20.62 GHz to 21.07 GHz). The input impedance is shown in Figure 28.

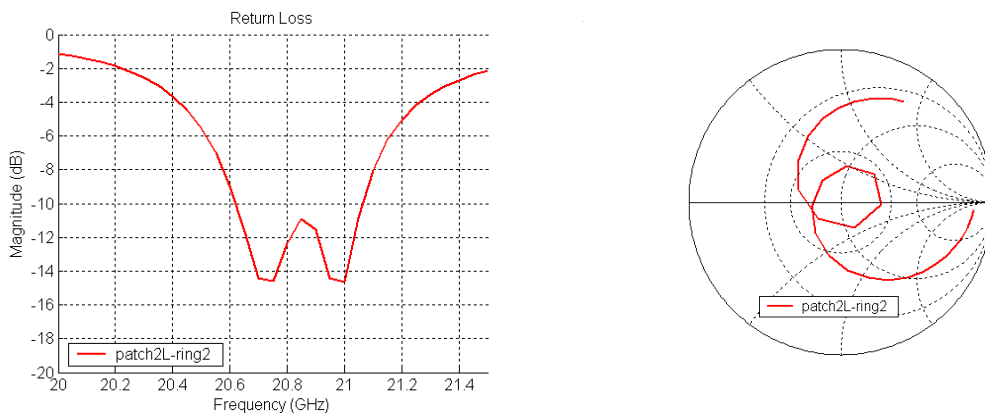


Figure 28. Input impedance of the inset fed patch antenna stacked with a square ring resonator

This result is obtained for the following dimensions, according to Figure 29.

- + Driven patch
 - $W = 2.7$ mm
 - $l = 0.85$ mm
 - $s = 0.109$ mm
- + Feeding line
 - $W_{70} = 0.132$ mm
 - $L_{70} = 1.55$ mm
 - $W_{50} = 0.274$ mm
- + Ring resonator
 - $W_{in} = 0.46$ mm
 - $W_{out} = 2.3$ mm

The inset length, l , is reduced compared to the one of a single patch, because the addition of a stacked resonator lowers the input impedance of the antenna. Then, as the quarter-wavelength transformer is kept unchanged, larger patch input impedance is required, and is obtained with a smaller inset feed.

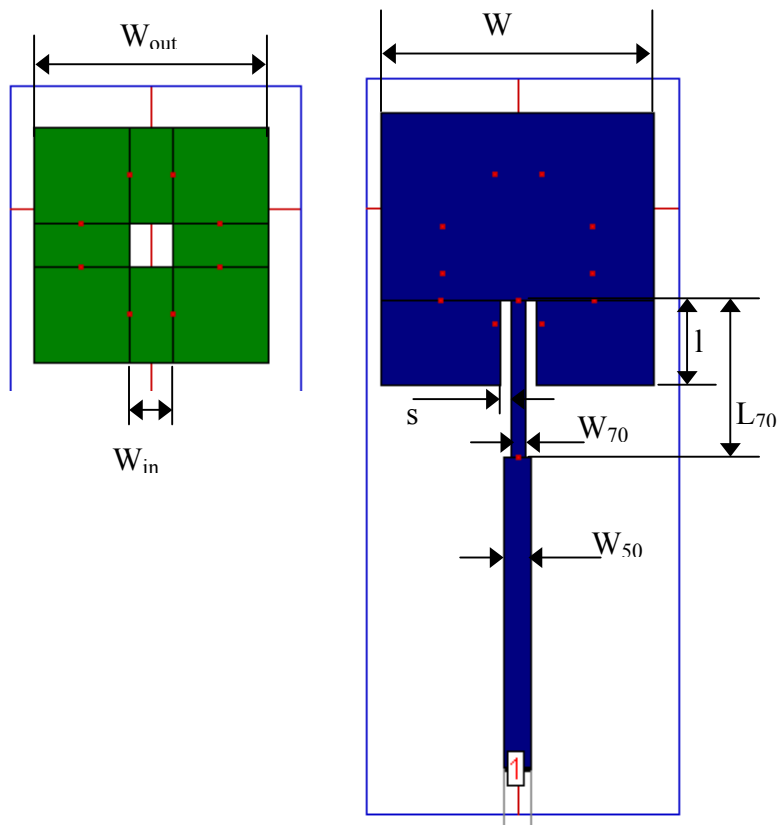


Figure 29. Geometry of the driven patch and the stacked square ring

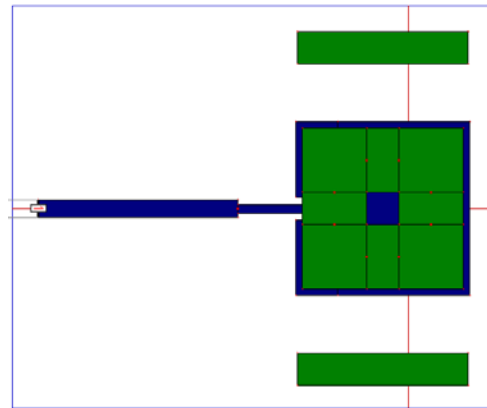
8.3.2. Patch with an inset feed stacked with a square ring coupled to parasitic elements

The parasitic elements are placed on the first layer, coupling directly to the stacked ring. The resonators are two microstrip strips placed symmetrically on both sides of the square ring, parallel to the feeding line. The insertion of the resonators on the top layer, directly coupled to the driven patch does not improve the impedance bandwidth. The geometry of the antenna is shown in Figure 13. The procedure to design these parasitic elements is as follows. First, the length of the resonators is chosen to be a half-wavelength. The width is chosen to be narrow to ensure that no orthogonal modes can be excited, and to not increase too much the overall width of the radiating element. Then, an optimization is carried out to obtain the largest possible impedance bandwidth. During this process, the dimensions of the other resonators, the square ring and the driven patch, need to be adjusted to compensate for the additional coupling introduced by the parasitic elements. Finally, the best result in terms of impedance is obtained with the following configuration, according to Figure 30. Again, the addition of the resonators lowers the input impedance of the antenna, and the inset length needs to be reduced for impedance compensation.

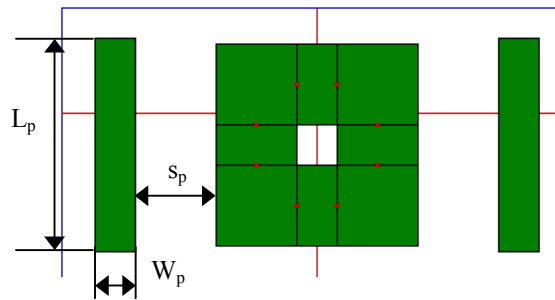
- + Driven patch
 - $W = 2.7 \text{ mm}$
 - $l = 0.65 \text{ mm}$
 - $s = 0.109 \text{ mm}$
- + Feeding line
 - $W_{70} = 0.132 \text{ mm}$
 - $L_{70} = 1.55 \text{ mm}$
 - $W_{50} = 0.274 \text{ mm}$
- + Ring resonator
 - $W_{in} = 0.5 \text{ mm}$
 - $W_{out} = 2.5 \text{ mm}$
- + Parasitic elements
 - $W_p = 0.5 \text{ mm}$
 - $L_p = 2.64 \text{ mm}$
 - $s_p = 1.0 \text{ mm}$

With only one port, the antenna exhibits an impedance bandwidth of 3.35% around a centre frequency of 20.85 GHz (20.5 GHz to 21.2 GHz), as shown in Figure 31. The addition of a second port affects the input impedance versus frequency response. The coupling between the two ports is between -25 dB and -20 dB within the above cited bandwidth. Another optimization process is required to improve the bandwidth. Nevertheless, the modification of the patch geometry modifies the radiation patterns of the radiating element, and a good circular polarisation could not be achieved.

a) The radiating element



b) The resonators on the first layer



c) CP configuration

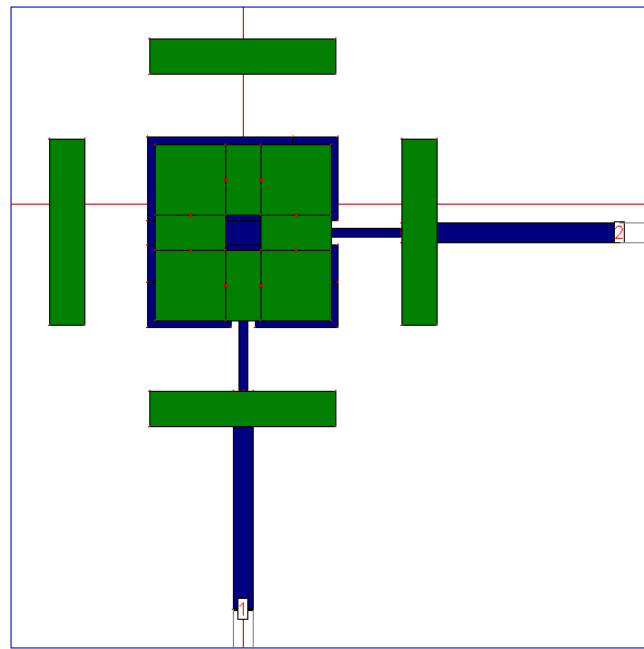


Figure 30. Patch antenna stacked with a ring resonator and coupled to parasitic elements

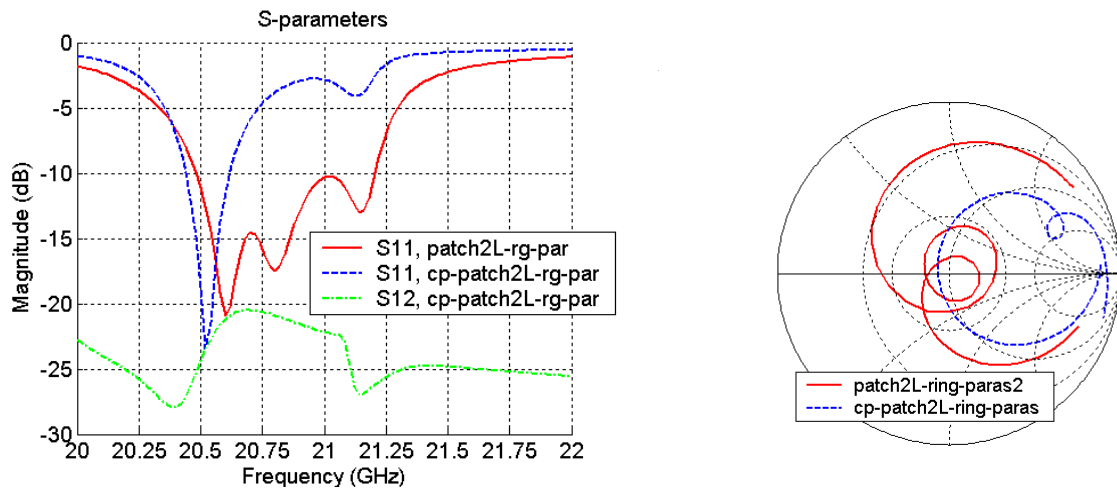


Figure 31. Input impedance of the patch antenna stacked with a ring resonator and coupled to parasitic elements

8.4. Annex 4: Summary of the element dimensions for radiating elements on three-layer LTCC substrate

8.4.1. Single port configuration

Table 10 : Dimensions of the resonating elements, and impedance bandwidth of antennas with a single feed

Configuration	Square patch	Transformers	Square ring	Parasitic elements	Bandwidth, F_o
Single patch	$W = 2.61$ mm	$W_{\text{transf1}} = 0.10$ mm $L_{\text{transf1}} = 1.65$ mm $W_{\text{transf2}} = 0.75$ mm $L_{\text{transf2}} = 1.50$ mm	/	/	0.97% 20.52 GHz
Patch + ring	$W = 2.61$ mm	$W_{\text{transf1}} = 0.10$ mm $L_{\text{transf1}} = 1.65$ mm $W_{\text{transf2}} = 0.45$ mm $L_{\text{transf2}} = 1.50$ mm	$W_{\text{out}} = 2.35$ mm $W_{\text{in}} = 0.67$ mm	/	1.94% 20.6 GHz
Patch + ring + parasitic elements	$W = 2.61$ mm	$W_{\text{transf1}} = 0.10$ mm $L_{\text{transf1}} = 1.65$ mm	$W_{\text{out}} = 2.35$ mm $W_{\text{in}} = 0.69$ mm	$W_p = 0.50$ mm $L_p = 2.60$ mm $s_p = 1.60$ mm	4.15% 20.73 GHz

8.4.2. Two-port configuration

Table 11 : Dimensions of the resonating elements, and impedance bandwidth of antennas with two feeds

Configuration	Square patch (mm)	Transformers (mm)	Square ring (mm)	Parasitic elements (mm)	2nd square ring (mm)	Bandwidth, Fo
Patch + ring	W = 2.61	W _{transf1} = 0.10 L _{transf1} = 1.65 W _{transf2} = 0.45 L _{transf2} = 1.50	W _{out} = 2.35 W _{in} = 0.67			2.19% 20.57 GHz
Patch + ring + parasitic elements	W = 2.61	W _{transf1} = 0.10 L _{transf1} = 1.65	W _{out} = 2.32 W _{in} = 0.70	W _p = 0.50 L _p = 2.60 S _p = 1.615		4.08% 20.82 GHz
Patch + ring + parasitic elements + ring *	W = 2.61	W _{transf1} = 0.10 L _{transf1} = 1.90	W _{out} = 2.4 W _{in} = 0.60	W _p = 0.50 L _p = 2.59 S _p = 1.40	W _{out} = 2.4 W _{in} = 0.65	5.31% 20.71 GHz

*: with a single port, only the dimensions of the transformer are different (W_{transf1} = 0.12 m, L_{transf1} = 1.80 mm).

8.4.3. The final radiating element with the feeding system

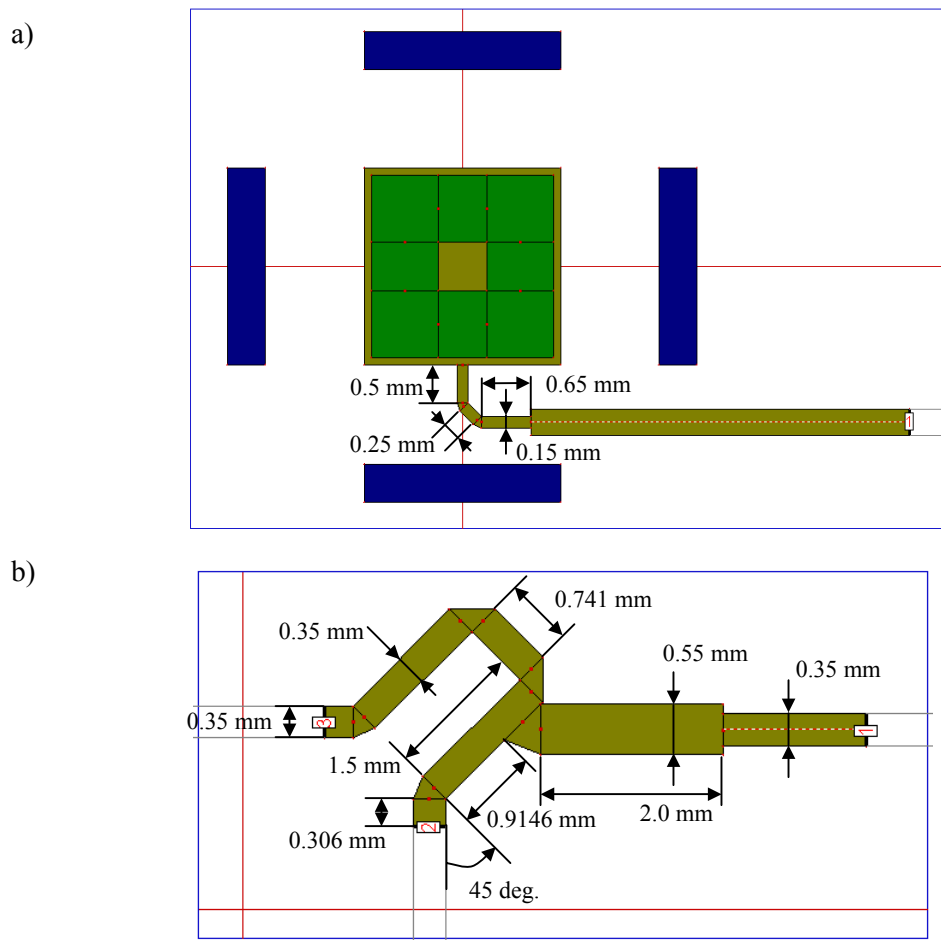


Figure 32. Radiating element with the transformer (a) and with the complete feeding circuit (b)

Table 12 : Dimensions of the resonating elements, and impedance bandwidth of the antennas with the feeding system

Configuration	Square patch (mm)	Transformers (mm)	Square ring (mm)	Parasitic elements (mm)	2 nd square ring (mm)	Bandwidth, Fo
Patch + ring + parasitic elements + ring	W = 2.61	W _{transf1} = 0.15 L _{transf1} = 1.515 (mean length)	W _{out} = 2.4 W _{in} = 0.60	W _p = 0.50 L _p = 2.59 S _p = 1.40	W _{out} = 2.4 W _{in} = 0.65	5.08% 20.675 GHz

UNCLASSIFIED

SECURITY CLASSIFICATION OF FORM
(highest classification of Title, Abstract, Keywords)

DOCUMENT CONTROL DATA

(Security classification of title, body of abstract and indexing annotation must be entered when the overall document is classified)

1. ORIGINATOR (the name and address of the organization preparing the document. Organizations for whom the document was prepared, e.g. Establishment sponsoring a contractor's report, or tasking agency, are entered in section 8.) Defence R&D Canada – Ottawa 3701 Carling Avenue Ottawa, On, K1A 0Z4		2. SECURITY CLASSIFICATION (overall security classification of the document, including special warning terms if applicable) UNCLASSIFIED	
3. TITLE (the complete document title as indicated on the title page. Its classification should be indicated by the appropriate abbreviation (S,C or U) in parentheses after the title.) DESIGN OF A MICROSTRIP FED CIRCULARLY POLARISED PRINTED ANTENNA FOR AN AEHF PHASED ARRAY (U)			
4. AUTHORS (Last name, first name, middle initial) Clénet, Michel			
5. DATE OF PUBLICATION (month and year of publication of document) June 2004		6a. NO. OF PAGES (total containing information. Include Annexes, Appendices, etc.) 40	6b. NO. OF REFS (total cited in document) 15
7. DESCRIPTIVE NOTES (the category of the document, e.g. technical report, technical note or memorandum. If appropriate, enter the type of report, e.g. interim, progress, summary, annual or final. Give the inclusive dates when a specific reporting period is covered.) Technical Memorandum			
8. SPONSORING ACTIVITY (the name of the department project office or laboratory sponsoring the research and development. Include the address.)			
9a. PROJECT OR GRANT NO. (if appropriate, the applicable research and development project or grant number under which the document was written. Please specify whether project or grant) 15ck18		9b. CONTRACT NO. (if appropriate, the applicable number under which the document was written)	
10a. ORIGINATOR'S DOCUMENT NUMBER (the official document number by which the document is identified by the originating activity. This number must be unique to this document.) DRDC Ottawa TM 2004-138		10b. OTHER DOCUMENT NOS. (Any other numbers which may be assigned this document either by the originator or by the sponsor)	
11. DOCUMENT AVAILABILITY (any limitations on further dissemination of the document, other than those imposed by security classification) <input checked="" type="checkbox"/> Unlimited distribution <input type="checkbox"/> Distribution limited to defence departments and defence contractors; further distribution only as approved <input type="checkbox"/> Distribution limited to defence departments and Canadian defence contractors; further distribution only as approved <input type="checkbox"/> Distribution limited to government departments and agencies; further distribution only as approved <input type="checkbox"/> Distribution limited to defence departments; further distribution only as approved <input type="checkbox"/> Other (please specify):			
12. DOCUMENT ANNOUNCEMENT (any limitation to the bibliographic announcement of this document. This will normally correspond to the Document Availability (11). However, where further distribution (beyond the audience specified in 11) is possible, a wider announcement audience may be selected.)			

UNCLASSIFIED

SECURITY CLASSIFICATION OF FORM

DCD03 2/06/87

13. ABSTRACT (a brief and factual summary of the document. It may also appear elsewhere in the body of the document itself. It is highly desirable that the abstract of classified documents be unclassified. Each paragraph of the abstract shall begin with an indication of the security classification of the information in the paragraph (unless the document itself is unclassified) represented as (S), (C), or (U). It is not necessary to include here abstracts in both official languages unless the text is bilingual).

This document reports the study of a circularly polarized printed antenna realised with LTCC material. This antenna is developed as a radiating element for a phased array with tile architecture for advanced EHF communication systems. Due to constraints imposed by the LTCC fabrication process and the application, techniques to improve the impedance bandwidth have been applied. These techniques are based on the proximity coupling of resonant structures to the driven antenna. The impedance bandwidth has been improved by a factor 5, and the required bandwidth for AEHF communications has been obtained. Arrays of four optimized radiating elements have been studied. The results are not satisfactory throughout the bandwidth, mainly due to the radiation of the microstrip feeding system required to generate the circular polarization. Another radiating element should be developed with a design suitable for an array for AEHF communications. A solution using the aperture-coupled technique to feed the radiating element can be applied to achieve this goal.

14. KEYWORDS, DESCRIPTORS or IDENTIFIERS (technically meaningful terms or short phrases that characterize a document and could be helpful in cataloguing the document. They should be selected so that no security classification is required. Identifiers such as equipment model designation, trade name, military project code name, geographic location may also be included. If possible keywords should be selected from a published thesaurus. e.g. Thesaurus of Engineering and Scientific Terms (TEST) and that thesaurus-identified. If it is not possible to select indexing terms which are Unclassified, the classification of each should be indicated as with the title.)

Antenna
Microstrip Patch
Bandwidth Enhancement
Circular Polarization
LTCC Technology
Array Antennas

Defence R&D Canada

Canada's leader in defence
and national security R&D

R & D pour la défense Canada

Chef de file au Canada en R & D
pour la défense et la sécurité nationale



www.drdc-rddc.gc.ca